4-15-1983

Derivation of the transformation relationship of pseudo-invariant features of two landsat images

Jeffrey R. Sefl

DERIVATION OF THE TRANSFORMATION RELATIONSHIP OF PSEUDO-INVARIANT FEATURES OF TWO LANDSAT IMAGES

by

Jeffrey R. Sefl

A thesis submitted in partial fulfillment
of the requirements for the degree of
Bachelor of Science in the School of
Photographic Arts and Sciences in the
College of Graphic Arts and Photography
of the Rochester Institute of Technology

Signature of the Author.....Jeffrey R. Sefl.....
Photographic Science and
Instrumentation Division

Certified by.....John P. Arheirt.....
Thesis Advisor

Accepted by.....Ronald Frarini.....
Supervisor, Undergraduate Research

ROCHESTER INSTITUTE OF TECHNOLOGY

COLLEGE OF GRAPHIC ARTS AND PHOTOGRAPHY

PERMISSION FORM

Title of thesis DERIVATION OF THE TRANSFORMATION RELATIONSHIP OF PSEUDO-INVARIANT FEATURES OF TWO LANDSAT IMAGES.

I, Jeffrey R. Sefl, hereby grant permission to Wallace Memorial Library, of R.I.T. to reproduce my thesis in whole or in part. Any reproduction will not be for commercial use or profit.

Date: 4/15/83

Signature of Author Jeffrey R. Sefl

DERIVATION OF THE TRANSFORMATION RELATIONSHIP OF PSEUDO-INVARIANT FEATURES OF TWO LANDSAT IMAGES

by

Jeffrey R. Sefl

Submitted to the
Photographic Science and Instrumentation Division
in partial fulfillment of the requirements
for the Bachelor of Science degree
at the Rochester Institute of Technology

ABSTRACT

The purpose of this effort was to determine the relationships of the spectral radiance distributions of pseudo-invariant features for a selected pair of Landsat images. The relationships for the four bands (band 4 through band 7) were determined to be linearly related. The transformation equations will map one images brightness values on to a second images brightness values.

ACKNOWLEDGEMENTS

The author wishes to express special gratitude to Dr. John R. Schott of the Rochester Institute of Technology who supplied equipment, ideas, and his own time towards the completion of this thesis.

Acknowledgement also go to Ned Schimminger for devoting his time and efforts to help solve many of the problems encountered while working with the Digital Equipment Corporation PDP-11/23 computer.

DEDICATION

This work is dedicated to the author's parents, who gave the opportunity and support needed to succesfully complete this thesis.

TABLE OF CONTENTS

LIST OF TABLES

Tables

LIST OF FIGURES

Figure

LIST OF SYMBOLS

b	y intercept of straight line, 10
B#1	band # of image 1 (#= 4,5,6 or 7), 35
B#2	band # of image 2 (#= 4,5,6 or 7), 35
B#C	band # of transformed image using relationships determined by the linear histogram operation, 35
B#E	band # of transformed image using relationships determined by regession analysis, 35
CCT	computer compatible tape, 1
CRT	cathode ray tube, 9
D	density, 25
H	exposure, 25
IBM	International Business Machines
LHAO	linear histogram analysis operation, 11
m	slope of a straight line, 10
MSS	multispectral scanner system, 1
NASA	National Aeronautical and Space Administration, 1
PIF's	pseudo-invariant features, 2
R	reflectance, 25
s	standard deviation, 10
SCS	Scene Color Standard technique, 3
um.	micrometers, 1
$\bar{X}$	mean, 10

α absorptance, 25

β integrated scattering coefficient, 25

I. INTRODUCTION

The impetus for this research is the Gypsy Moth problem in the United States, although the research will be applicable to other research that deal with Landsat imagery. See Appendix A for the history of the Gypsy Moth problem.

The Landsat series of Earth Resources Technology Satellites provide users with a wealth of knowledge. Landsat images are used to assess crops, urban growth, land formations, etc..

Landsat-1 MSS tapes are generated by a four band scanner operating in the spectral region of 0.5 to 1.1 um..

There are six detectors for each band (bands 4 through 7) which scan perpendicular to the flight path of the satellite. The resulting signal from each detector is encoded and transmitted to a receiving station where it is recorded. The data is then processed by NASA converting the data into binary form. The data are then stored on magnetic tapes (CCT). A Landsat image consists of approximately 3296 X 3296 pixels of information. A pixel has associated with it four brightness values, one for each band. The brightness values for bands 4 through 6 range in value from 0, which corresponds to black in the image, to 127 which corresponds to white. The range in brightness value in band 7 is 0 to 63.[1,1]

In order to enhance Landsat imagery it is necessary to be able to directly relate two or more image's brightness distributions.[3,4]

The purpose of this thesis work was to: (1), isolate a portion (window) of a Landsat scene, by reading the brightness values recorded on Landsat computer-compatible tapes (CCT). This portion or window will be comprised of pixels (image elements) which will be either variant features (features who's brightness values are subject to change with time, i.e. water, foliage, etc.) or pseudo-invariant features, abbreviated PIF's (features who's brightness values are not subject to change with time, i.e. concrete, asphalt, etc.). The window is spectrally filtered, by investigating the ratio of band 7 to band 5, to isolate only PIF's; and (2), derive a mathematical relationship that relates one set of Landsat image PIF's brightness values to another set of Landsat image PIF's brightness values. The mathematical relationship will map one image's PIF's brightness values on to the second image's PIF's brightness values is derived. The relationship derived can be used to photometrically calibrate, display decalibrate, or modify the images in various ways such that the original images are enhanced, thereby increasing the information content of the images.[1] Once the relationship

II. LITERATURE REVIEW

One method of enhancement of imagery is the ability to subtract from the image data changes in recorded reflectance due to the scattering and absorption of radiant energy in the atmosphere. By doing this, two images that were recorded on different dates, under different atmospheric conditions may be directly compared.[1,2,4] Since the spectral radiance recorded in a Landsat image is directly proportional to the spectral reflectance of the objects imaged, it will be important to remove the atmospheric effects for quantitative analysis of the imagery.[2]

In 1974, Peich and Schott[5] published a paper describing a theory of correcting fo atmospheric effects on satellite images. Data processing was accomplished through microdensitometry of the shadow areas located within the image. Walker [6], et al (1977), determined that if Landsat imagery is not photometrically calibrated, only relative stress maps could be generated to assess gypsy moth defoliation levels. Unless the images were calibrated photometrically, interpretations relative to the significance of temporal changes of stress patterns were questionable. Attempts were made to use Calspan's Scene Color Standard (SCS) technique (see Appendix B) to calibrate Landsat images photometrically. This technique is not

feasible because it would require at least one full pixel to be in shadow. A pixel in a Landsat image is approximately 79 meters square, which is a very large area to be totally in shadow. Attempts were made to use shadows created by clouds located within the image, but cloud densities varied considerably so further investigation was discontinued.[7] Nelson[8] (1982), determined that of three data tranformations investigated (differencing, ratioing, and differencing of ratios), the best method for delineation of forest change due to gypsy moth activity is the differencing of ratios. Ratioing of bands (band 7/band 5; band 7, reflected infrared, 0.8 to 1.1 um., and band 5, red, 0.6 to 0.7 um.) minimizes atmospheric effects but does not remove them. The reason the effects are not removed is that the attenuation of the recorded brightness values is different for each spectral band.

It is important to determine what type of relationship exists between two landsat image's PIF's recorded brightness values. A Landsat image can be calibrated using underflight images (images of the same scene recorded at a lower altitude). The spectral radiance recorded in a Landsat image is proportional to the spectral reflectance recorded in an underflight image of the same scene.[4] The underflight image can be calibrated for atmospheric effects, digitized, and related through mathematical relationships to

the Landsat image (this research has not been done). The atmospheric effects can now be accounted for in the Landsat image. If two Landsat images can be related through transformation equations that map one image's brightness values on to the second image's brightness values, then the atmospheric effects can be accounted for in each scene. This obviates the need to calibrate each Landsat image using underflight data. This would be an efficient and cost effective method for calibrating Landsat imagery.

III. EXPERIMENTAL

The first objective of this thesis was to isolate portions of Landsat images; then filter out variant features leaving only PIF's. A Fortran program was written to be used on a Digital Equipment Corporation PDP-11/23 computer (see Appendix C). The program will isolate up to a 20 pixel X 20 pixel window, and remove variant features leaving only PIF's.

The program lists the header information on the tape containing the date the image was taken, the location of the image in longitude and latitude, the sun azimuth angle, the sun elevation, the scene identification number, and which satellite recorded the image (one, two, or three). (See Appendix D for a flow chart description of THESIS.FTN.)

The window location and size are chosen. To locate the window in the desired portion of the image one chooses X and Y coordinates. The program will prompt the user to choose a line number, strip number, and window size. The line number corresponds to the Y direction, or the direction of the scan lines. The strip number corresponds to a particular quarter of the image (Landsat-1 images consist of four columns 824 pixels wide by 3296 pixel long). The window size determines the size of the output matrix.

The program then files forward to the strip chosen. At this point a column number up to the limit specified by the image parameters is chosen. The limit of the choice is based on the size of the window chosen. Since the image is 3296 pixels wide and this is divided into four columns, the width of each column is 824 pixels. If a column number less than 1 or greater than 824 minus the window size is chosen, erroneous data will be generated. This is due to the boundaries that separate the four columns in the image.

The program prints the line number, column number, strip number, and window size. The unfiltered window is displayed in four separate bands. After the unfiltered window is displayed the operator enters the parameters to reject variant pixels. The ratio of bands 7/5 is used to isolate PIF's. This is due to the spectral distibutions of the types of features (see Figure 1). Variant features have a high infrared to red ratio due to there spectral reflectance. The parameter for water rejection are also entered for bands 5 and 7. Pixels who's ratios are not within the limits set for the ratio are rejected as are those who's brightness values for bands 5 and 7 are less than the limits set for water rejection.

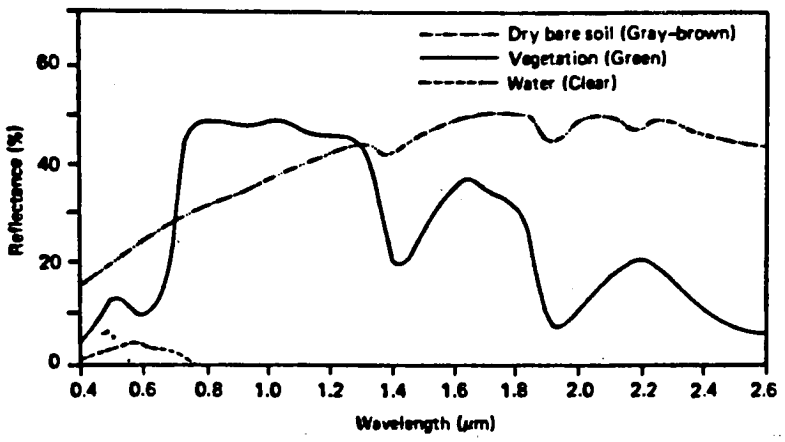

Figure 1. Spectral signatures for variant elements.

The window is filtered and then displayed. The display is in the form of 4 matrices, (one for each band) of zeroes and brightness values. Zeroes correspond to variant features and the brightness values correspond to PIF's (see Appendix E for a sample printout).

Two Landsat scenes located over central Maine were selected for the analysis. One image was recorded on August 22, 1974, scene Id.# 10760-14445, and the second scene was recorded on May 31, 1976, scene Id.# 11408-14101.

The locations of two urban areas were identified in the images. There is a large probabilty that PIF's are located in these areas. This is because, urban areas contain things that are considered pseudo-invariant such as, concrete

buildings, driveways, or asphalt roads, etc.. These things are considered to be PIF's because their reflectances do not change very much over long periods of time. The locations (coordinates) of the two areas were found by imaging 512 X 512 pixel portions of the Landsat scenes on a DeAnza Image Display System. The DeAnza system is capable of reading a 512 X 512 pixel section from a Landsat CCT, and displaying a color composite image on a CRT. Sections of the displayed image can be magnified which aid in both locating the exact coordinates of PIF's and determining the pixel rejection parameters.

The parameters for pixel rejection were determined by imaging the coordinates of a chosen window on the DeAnza system, drawing the outlines of roads and an airport runway directly from the CRT on to the printout of the unfiltered window. The ratio of the printed brightness values for band 7/5 were determined for water, variant features, and PIF's. The mean and the range of the ratio for PIF's were determined. The values for water were read directly from the printout of the window. This technique was used to determine the parameters for both Landsat images. Several windows were located in each image and filtered. Windows were located over forested areas, water, and areas that contained both water and foliage, in each image to test how well the parameters filtered the data.

The brightness values for each band recorded in the filtered windows were entered into two data sets on the IBM 370 computer system. The data sets consisted of the brightness values isolated for each band. Statistical Analysis System[9] was used to analyze the data. Two methods of analyses to determine the relationship of the two Landsat image's PIF's were used. The data was sorted in ascending order for each band and a least squares regression analysis was performed regressing one image's PIF's brightness values on the second image's (bands 4 through 7). This was one method of determining the relationship between the image's PIF's features. The second method relates the means and the standard deviations of the two image's PIF's brightness values. Histograms were generated from the data sets, one for each band. The means and the standard deviations were determined for each band in both of the images. The two data sets were related in the following manner:

the slope of the line (m) = s1/s2,

the intercept of the line (b) = $\bar{X}1 - \bar{X}2$ (s1/s2)

where,

s1 and s2, are the standard deviations of the two image's recorded brightness values,

$\bar{X}1$ and $\bar{X}2$, are the means of the two image's recorded brightness values.

This method is a linear histogram analysis operation (LHAO) based on the premise that the histograms are only different by a linear operation.

Histograms were generated from the resultant transformations. A Chi square goodness of fit test was done to test how well the transformation equations mapped one image's brightness values on to the second image's brightness values.[9-11]

IV. RESULTS

Several windows were isolated using the Fortran program described in the previous section. The parameters used to isolate PIF's are listed in Table 1.

Table 1. Parameters for pixel rejection.

	Upper Ratio	lower Ratio	Cut off values for water	
			band 5	band 7
Image 1	0.8	0.3	15	11
Image 2	0.65	0.35	16	12

where, image 1 corresponds to the August 22, 1974 Landsat scene and,

image 2 the May 31, 1976 Landsat scene.*

The recorded brightness values in bands 5 and 7 are used to reject water.

Several windows were isolated in each image and filtered using the values listed in Table 1. A total of 324 brightness values for each image's bands were entered into

*Note: the notation for image identification listed above will be used throughout this paper.

two data sets for analysis on the IBM 370 computer. The values were regressed for each corresponding band (bands 4 through 7). The means and standard deviations were calculated for each bands brightness values (see Appendix F for a listing). The slopes and intercepts for the transformation equations were determined using the two techniques previously described (see Table 2).

Table 2. Slopes and intercepts of transformation equations.

	Methods used			
	Regression		LHAO	
	slope	intercept	slope	intercept
Band 4	0.66037	10.5696	0.6249	9.7251
Band 5	0.7499	2.4749	0.7658	1.9309
Band 6	0.7864	1.8818	0.8196	0.4963
Band 7	0.9447	-1.051	0.8685	0.2819

All parameters listed in Table 2 were determined to be significant using 90% confidence limits.

The slopes and intercepts were determined so as to map the PIF's bightness values of image 2 on to the PIF's brightness values of image 1. Histograms were generated for both image's PIF's brightness values, and for the PIF's brightness values of the transformed image.

A Chi square goodness of fit test was performed to test how well the transformed data sets hostogram approximated the histogram of image 1.

The standard error was calculated for the two methods of transforming the images (see Table 3).

Table 3. Listing of standard errors.

	Method	
	Regression	LHAO
Band 4	0.74	0.51
Band 5	0.78	0.72
Band 6	1.34	0.96
Band 7	0.62	0.52

The transformed data's histograms were tested for goodness of fit. The null hypothesis was that the two image's frequency distribtions came from the same population and the alternative was that they did not come from the same population. The null hypothesis rejected at an alpha value of 0.10. There are several reasons that could cause this to happen. The errors associated with the transformations could shift the transformed data's histogram enough to cause the goodness of fit test to fail, or there are variant

feature's brightness values in the data sets (see Appendix F for histograms, means, and standard deviations).

V. DISCUSSION

The results of the regression analysis and the LHAO analysis were similar. The greatest difference between their slopes and intercepts were in bands 6 and 7. The standard error for band 6 was larger than those for bands 4,5, and 7. This is most likely due to mixed pixels (pixels that contain both variant and pseudo-invariant features) being included in the data sets analyzed. The standard error is an estimate of the overall variation in the transformation equations. The equations map image 2's PIF's brightness values on to image 1's PIF's brightness values to within $\pm$ 1 brightness count. The errors in the recorded brightness values in a Landsat image are approximately 50% of a brightness count. The standard errors (worst case) are approximately twice the inherent error in the recorded brightness values in a Landsat image. In terms of reflectances of objects, the overall variation in there recorded reflectances would be approximately $\pm$ 0.2 reflectance units.

The better method of determining the transformation equations, based on the standard errors for the two methods, is the LHAO analysis.

VI. CONCLUSIONS

This experiment resulted in the conclusion that there is a linear relationship between two Landsat image's PIF's brightness values (for the same scene) based on the regressions being significant.

Suggestions for future work include the investigation of creating mathematical algorithms that better isolate PIF's in images including models that account for images recorded throughout various seasons of the year. Other areas of future investigation include; using the transformation theory to detect changes in PIF's by differencing the original image data with the transformed image's data , and investigating the differences of deriving transformation equations using small sample sizes from registered images versus large sample sizes from unregistered images.

VII. REFERENCES

1 [illegible]hy, M.C., "Generation of Software to Produce a Landsat Scene Comprised Only of Pseudo-Invariant Features", B.S. Thesis, Rochester Institute of Technology, Rochester, N.Y., 1982.

2. Slater, P.N., Remote Sensing: Optics and Optical Systems, Addison-Wesley, U.S.A, 1980.

3. Castleman, K.R., Digital Image Processing, Prentice-Hall, New Jersey, 1979.

4. Lillesand, T.M., and R.W. Kiefer, Remote Sensing and Image Interpretation, Wiley & Sons, U.S.A., 1970.

5. Piech, K.R., and J.R. Schott, "Atmospheric Corrections for Satellite Water Quality Studies", Proceedings of the Society of Photo-Optical Instrumentation Engineers, Palos Verdes Estates, California, 1974.

6. Walker, J.E., et al, "Forest Damage Assessment System Study (FORDAS)", Calspan Technical Report, Report No. RK-6099-M-1, 1977.

7. Schott, J.R., Personal Communication, Tuesday, October 12, 1983.

8. Nelson, R.F., "Detecting Forest Canopy Changes Using Landsat", Report No. TM83918, RR-G2 04258, NASA/Goddard Space Flight Center, 1982.

9. Ray, A.A., et al, "Statistical Analysis System", SAS Institute Inc., United States, 1982.

10. Draper, N.R., and H. Smith, Applied Regression Analysis, Wiley & Sons, U.S.A., 1981.

11. Montgomery, D.C., and E.A. Peck, Introduction to Linear Regression Analysis, Wiley & Sons, U.S.A., 1982.

12. Rickmers, A.D., and H.N. Todd, Statistics an Introduction, McGraw-Hill, United States, 1967.

13. McRea, J.C., "Homeowner Attitudes Toward the Gypsy Moth and Control Efforts and Implications for Control Policy", Masters Thesis, S.U.N.Y. College of Environmental Science and Forestry, Syracuse, N.Y., 1973.

14. Rohde, W.G., and H.J. Moore, "Forest Defoliation Assessment with Satellite Imagery", Proceedings of the Environmental Research Institute of Michigan, 9th International Symposium on Remote Sensing of Environment, 1974.

15. Williams, D.L., et al, "Development of a Statewide Landsat Digital Data Base for Forest Insect Damage Assessment", Proceedings of the AutoCarto 5/ISPRS IV Symposium, Crystal City, Virginia, 1982.

16. Williams, D.L., and M.L. Stauffer, "A Forester's Look at the Application of Image Manipulation Techniques to Multitemporal Landsat Data", Machine Processing of Remotely Sensed Data Symposium, West Lafayette, Indiana, 1979.

17. Williams, D.L., "Computer Analysis and Mapping of Gvpsy Moth Defoliation Levels in Pennsylvania Using Landsat-1 Digital Data", NASA Earth Resources Survey Symposium, Houston, Texas, 1975.

18. Gaucher,D., et al, "Applications of Photometric Processes in Monitoring Vegitation Damage Due to External Stresses", Calspan Report, Buffalo, N.Y..

19. Williams, D.L., and B.J. Turner, "Computer Analysis and Mapping of Gypsy Moth Defoliation Levels in Northeastern Pennsylvania Using ERTS-1 Data", Office for Remote Sensing of Earth Resources Space and Engineering Laboratory, Pennsylvania State University, University Park, Pennsylvania, 1974.

20. Williams. D.L., and K.J. Ingram, "Integration of Digital Elevation Model Data and Landsat MSS Data to Quantify the Effects of Slope Orientation on the Classification of Forest Canopy Condition", Machine Processing of Remotely Sensed Data, West Lafayette, Indiana, 1981.

21. Nelson, R.F., "Defining the Temporal Window for Monitoring Forest Canopy Defoliation Using Landsat", The American Society of Photogrammetry, 47th Annual Meeting, Washington, D.C, 1981.

22. Schott, J.R., et al, "Photometric Derivation of Analytic Parameters for Assessment and Monitoring Over Extensive Areas of Stand Susceptibility to Bark Beetle Induced Tree Mortality", Calspan Research Proposal, 1980.

VIII. APPENDICES

APPENDIX A. History of the Gypsey Moth

The gypsy moth, Lymanthria Dispar (L.), was introduced into the United States in 1869. A French naturalist was conducting experements with the gypsy moth and silk worm in an attempt to create a hybrid for commercial use when it was accidentally released into the environment. By 1890, the gypsy moth had established itself. By 1973, gypsy moth infestation was detected in nine states.[8,13]

The moth, in its larval stage weakens or kills hundreds of thousands of acres of timber each year. Tree mortality can be directly attributed to defoliation by the gypsy moth larvae or by subsequent problems arising from the tree's weakened state. It defoliates many nothern hardwoods, favoring oaks, aspen and birches; conifers may also be attacked if the epidemic is severe. A single defoliation can kill white pine, spruce, and hemlock, while two defoliations are sufficient to kill most hardwoods.[8,13,21]

Control practices which include the application of pesticides, pheremones, microbial or viral insecticides, and the release of natural predators or sterilized male moths, depend on accurate and timely detection and location of areas supporting large populations of the gypsy moth.[13]

Present techniques of monitoring the extent and severity of gypsy moth defoliation include ground surveying, aerial sketchmapping, and air photointerpretation. These methods have proven to be expensive, inaccurate, and logistically unwielding. Landsat data does provide a more cost effective and efficient method of defoliation assessment.[14-22]

APPENDIX B. Scene Color Standard

On a clear day there are two illumination sources present, sun and scattered light from the atmosphere. Objects are illuminated by both or by only the hemispheric illumination (i.e. shadows). When a shadow falls on a surface that is illuminated by sun-plus-sky as shown in Figure 3, it provides images that can be used to compare the relative contribution of non-object radiance to the total radiance from any object in the scene. The theory and mathematics relating to the derivation are found in References 5 and 22. This parameter is called Beta (β), and it can be determined by measuring the density of eight to ten objects recorded on film) both in and out of shadow (i.e. a concrete driveway in partial shadow). The densities are transformed through the D-log H curve of a film to exposure. The relationship of exposure to reflectance is,

$$\text{Exposure (H)} = \propto \text{Reflectance (R)} + \beta \quad \text{or,}$$

$$H = \propto R + \beta .$$

Beta is the average energy value scattered into the optical path between the sensor recording material and the ground.

The other parameter, Alpha (α), must be determined before the total radiance recorded by the sensor can be

corrected to object reflectance. Alpha is the product of sun-plus-sky illumination multiplied by the total attenuation factor in the atmospheric path. References 5 and 22 provide the theory and mathematical derivation.

Once Alpha and Beta are known, the density of any image in the scene can be measured and corrected to the object's spectral reflectances on the ground.[18]

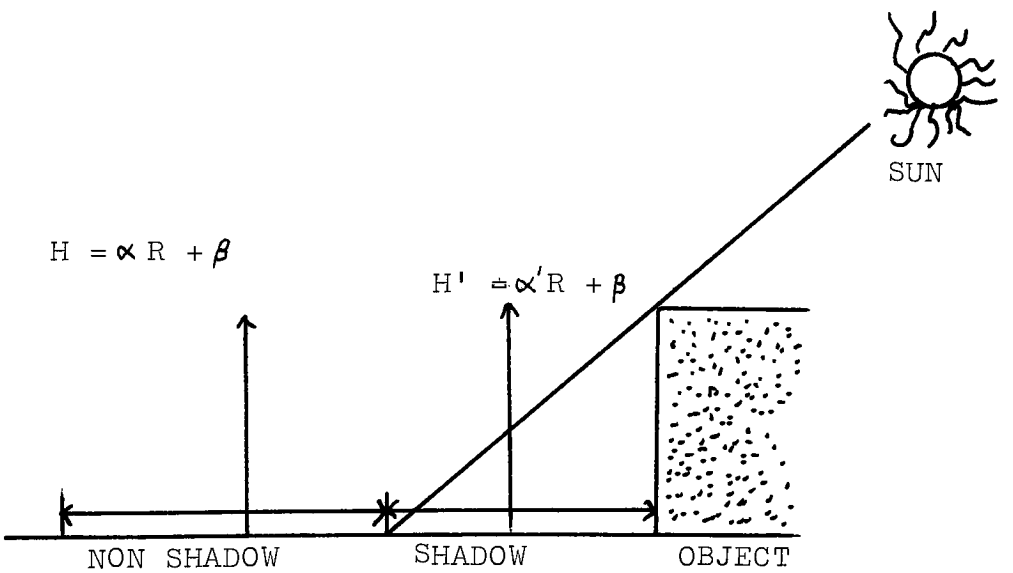

Figure 3. Key to photometric calibration.

APPENDIX C. THESIS.FTN computer program listing

```
C       THIS PROGRAM IS DESIGNED TO TAKE A N X N WINDOW FROM A
C       LANDSAT  IMAGE AND REMOVE VARIANT PIXELS LEAVING ONLY
C       INVARIANT PIXELS. IT WILL THEN PRINT OUT THOSE REMAINING PIXELS
C       IN EACH BAND. IT WILL ALSO, STORE THEM ON A MAGNETIC DISK.
        IMPLICIT INTEGER*2 (A-Z)
        REAL*4 MAXR,MINR,MIN4,MIN5,MIN6,MIN7,MV,M7,UPL,LOL
        REAL*4 RATIO6,RATIO7,RATIO,BNIR,BFIR,BRED
        INTEGER*2 LTBLOK(4),ISTS(2)
        LOGICAL*1 RED(824),GREEN(824),NIR(824),FIR(824),TIM(824)
        LOGICAL*1 BUFFER(3298),FILENM(5),ARRAY(40,40)
        ISTS(1)=0
        ISTS(2)=0
        DATA FILENM/'C','O','L','O','R'/
C       OPENS FOUR DISK FILES
        CALL LT4DRS(FILENM,824,ISTS)
C       START UP PROCEDURE FOR TAPE
        CALL LTSTRS(1,LTBLOK,ISTS)
        IF(ISTS(1).NE.0) GO TO 900
 2      CALL LTHRRS(LTBLOK,ISTS)
C       HEADER READ
        CALL L4RWRS(LTBLOK,ISTS)
        WRITE(7,*)'DO YOU WANT TO INSERT ANOTHER TAPE?'
        WRITE(7,*)'TYPE 1 FOR YES, AND 0 FOR NO.'
        READ(7,*)NT
        IF(NT.EQ.0)GOTO 1
        WRITE(7,*)'INSERT TAPE NOW.'
        WRITE(7,*)'HIT 1 TO CONTINUE.'
        READ(7,*)CC
        GOTO2
 1      WRITE(7,*)'DO YOU WANT TO OUTPUT ON SCREEN OR PRINTER?'
 0      WRITE(7,*)'TYPE IN 7 FOR SCREEN, OR 6 FOR PRINTER.'
        READ(7,*)CC
        WRITE(7,*)' WHAT LINE NUMBER DO YOU WANT? '
        READ(7,*) LN
        WRITE(7,*)' WHAT SIZE WINDOW DO YOU WANT (UP TO 20 A SIDE)?'
        READ(7,*) WSO
        WRITE(7,*)'WHICH STRIP DO YOU WANT? 1,2,3,OR 4'
        READ(7,*)N
        N=N-1
C       FILE FORWARD
        CALL LTFFRS(N,LTBLOK,ISTS)
C       READ HEADER
        CALL LTHRRS(LTBLOK,ISTS)
        WRITE(7,*)'WHAT COLUMN DO YOU WANT ?'
        WRITE(7,*)'YOU CAN CHOOSE A NUMBER UP TO',824-WSO,'.'
        READ(7,*) CN
        WRITE(7,*)'DO YOU WANT TO CHANGE ANY OF THE ABOVE  PARAMETERS ?'
        WRITE(7,*)'TYPE 1 FOR YES, AND 0 FOR NO.'
        READ(7,*)CH
        IF(CH.EQ.1)GOTO 1
        DO 10 I=1,LN-1
C       READ IMAGE RECORDS
        CALL LTRDRS(LTBLOK,BUFFER,ISTS)
 10     CONTINUE
        DO 20 J=1,WSO
        CALL LTRDRS(LTBLOK,BUFFER,ISTS)
C       UNPACKS RECORD
C       AND WRITES THEM INTO FOUR ARRAYS
        CALL LTUPRS(LTBLOK,BUFFER,GREEN,RED,NIR,FIR)
```

```
      WRITE(14'J)GREEN
      WRITE(15'J)RED
      WRITE(16'J)NIR
      WRITE(17'J)FIR
 20   CONTINUE
      WRITE(CC,*)'FIRST LINE NUMBER IS', LN
      WRITE(CC,*)'THE COLUMN NUMBER IS', CN
      WRITE(CC,25) WSO,WSO
 25   FORMAT('THE WINDOW SIZE IS',I3,'X',I3)
      WRITE(CC,*)'THE STRIP NUMBER CHOSEN WAS ',N+1
      WRITE(CC,90)
 90   FORMAT(////)
      DO 100 IBAND=4,7
      CALL OUTPUT(IBAND,WSO, CN,CC)
 100  CONTINUE
 500  CONTINUE
C     WRITE(7,*)'DO YOU WANT TO REWIND THE TAPE?( 1FOR YES,0 FOR NO )'
C     READ(7,*) RW
C     SETS PARAMETERS FOR PIXEL REJECTION
      WRITE(7,*)'CHOOSE AN UPPER LIMIT FOR THE RATIO.'
      READ(7,*)UPL
      WRITE(7,*)'CHOOSE A LOWER LIMIT FOR RATIO.'
      READ(7,*)LOL
C     SECTION THAT CREATES RATIOS OF CHOSEN BANDS
C     WRITE(7,*)'WHAT BAND DO YOU WANT TO RATIO?'
C     WRITE(7,*)'BAND 6 OR BAND 7.'
C     READ(7,*) BANDN
      WRITE(7,*)'CHOOSE A MINIMUM BRIGHTNESS VALUE FOR BAND 5.'
      READ(7,*)MV
      WRITE(7,*)'CHOOSE A MINIMUM BRIGHTNESS VALUE FOR BAND 7.'
      READ(7,*)M7
C     MIN4=MV
      MIN5=MV
C     MING=MV
      MIN7=M7
      WRITE(CC,90)
      DO 35 V=1,WSO
      READ(14'V)GREEN
      READ(15'V)RED
      READ(16'V)NIR
      READ(17'V)FIR
C     LOOPS THROUGH WINDOW
      DO 45 Z=1,WSO
      ARRAY(V,Z)=1
C
C     LOL= LOWER LIMIT
C     UPL= UPPER LIMIT
C     DELETES INVARIANT PIXELS
      BNIR=NIR(Z+CN)
      BFIR=FIR(Z+CN)
      BRED=RED(Z+CN)
C     IF ( BANDN.EQ.6) RATIO = BNIR/BRED
C     IF ( BANDN.EQ.7) RATIO = BFIR/BRED
C
C     RATIO6 = BNIR/BRED
      RATIO7 = BFIR/BRED
C     IF(RATIO6.GE.UPL.OR.RATIO6.LE.LOL)ARRAY(V,Z)=0
      IF(RATIO7.GE.UPL.OR.RATIO7.LE.LOL)ARRAY(V,Z)=0
C     IF(GREEN(Z+CN).LT.MIN4)ARRAY(V,Z)=0
      IF(RED(Z+CN).LT.MIN5)ARRAY(V,Z)=0
C     IF(NIR(Z+CN).LT.MING)ARRAY(V,Z)=0
      IF(FIR(Z+CN).LT.MIN7)ARRAY(V,Z)=0
 45   CONTINUE
 35   CONTINUE
      DO 65 IBAND=14,17
      WRITE(CC,*)'     BAND ', IBAND - 10
```

```
      DO 75 V=1,WSO
C     TIM IS THE FILE OF FILTERED ARRAY OF PIXELS
C     WHICH WILL BE PRINTED
      READ(IBAND'V)TIM
      DO 85 M=1,WSO
      IF(ARRAY(V,M).EQ.0) TIM(M+CN)=0
 85   CONTINUE
      WRITE(CC,70)V,(TIM(Z+CN),Z=1,WSO)
 70   FORMAT('   LINE',I3,4X,40I3)
 75   CONTINUE
 65   CONTINUE
C     IF (RW.EQ.1)CALL LTRWRS(LTBLOK,ISTS)
      STOP
      END
C
C     PRINTS UNFILTERED WINDOW
C
      SUBROUTINE OUTPUT(IBAND,WSO,CN,CC)
      IMPLICIT INTEGER*2 (A-Z)
      LOGICAL*1 OUTAR(824)
      WRITE(CC,*)' BAND ',IBAND
      W=1
      LUNIT=10+IBAND
      DO 100 J=1,WSO
      READ(LUNIT'J)OUTAR
C     X MOVES IN THE X DIRECTION
      WRITE(CC,70)W,(OUTAR(X),X=CN,CN+WSO-1)
 70   FORMAT('  LINE ',I3,4X,40I3)
      W=W+1
 100  CONTINUE
      RETURN
      END
```

APPENDIX D. Flow chart description of THESIS.FTN

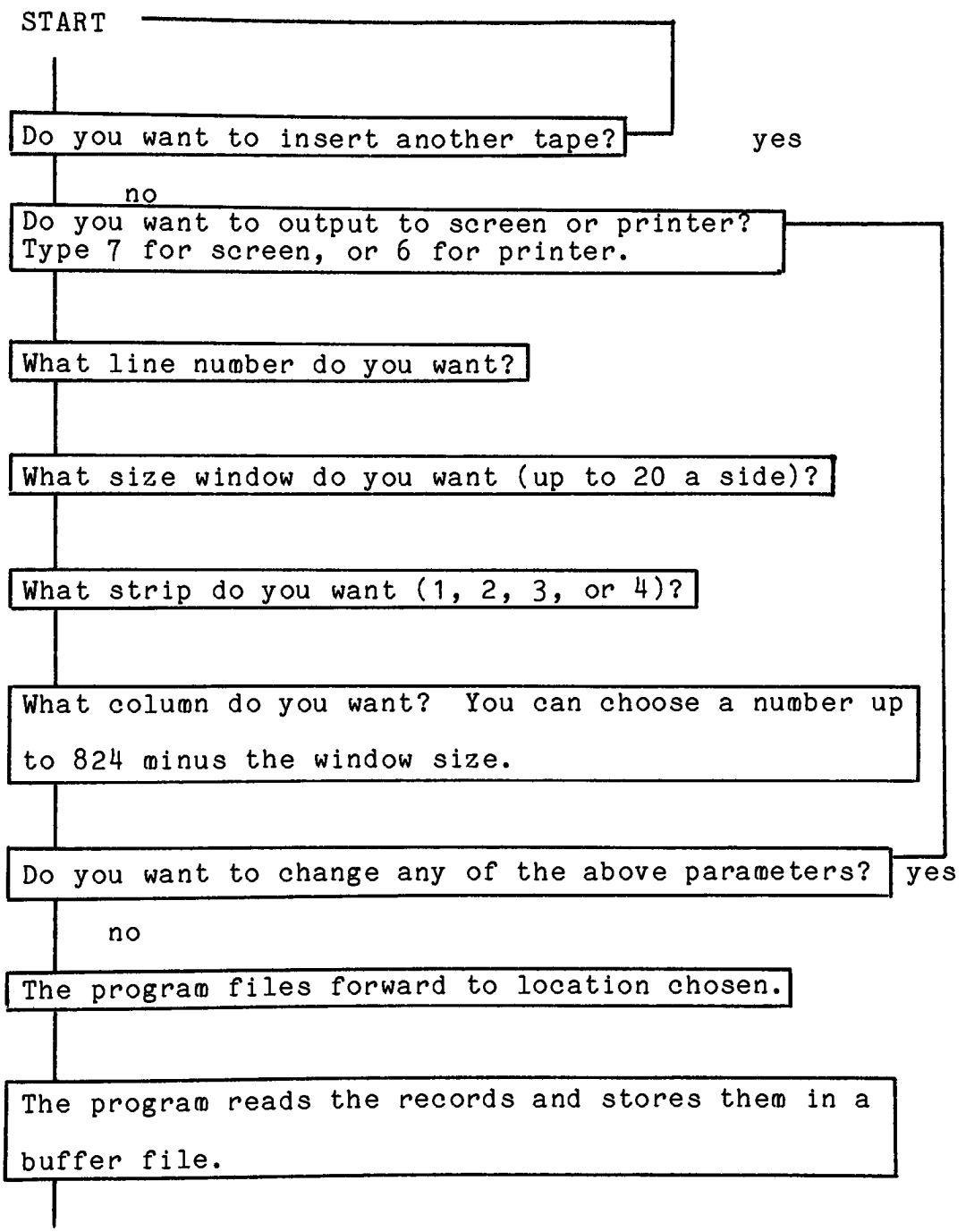

Figure 4. Flow chart description of THESIS.FTN.

Figure 4. continued

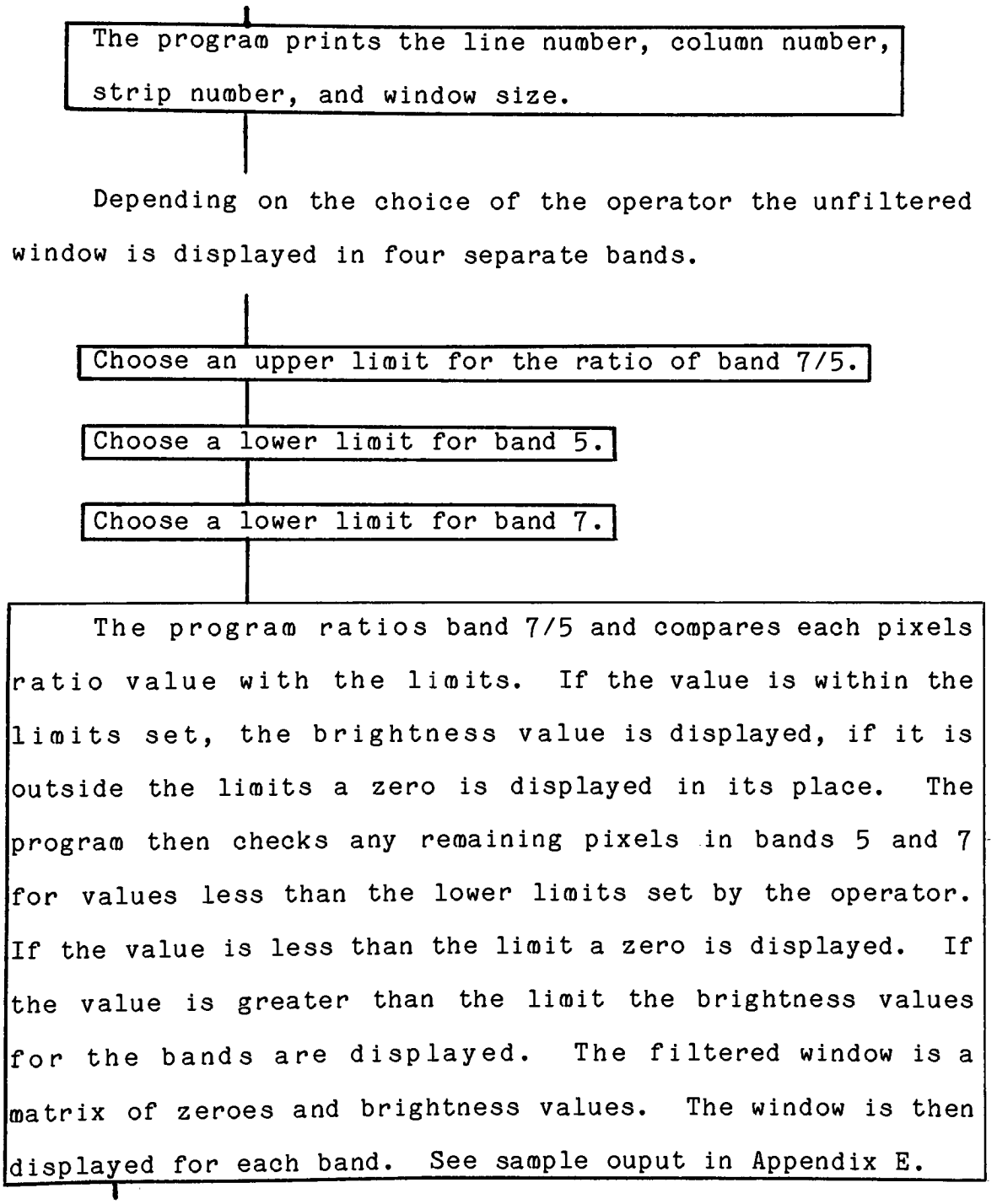

APPENDIX E. Sample output of THESIS.FTN

```
 FIRST LINE NUMBER IS    1550
 THE COLUMN NUMBER IS     361
 HE WINDOW SIZE IS 20X 20
 THE STRIP NUMBER CHOSEN WAS        3

 BAND          4
 LINE     1     35 35 37 40 42 44 44 44 44 46 44 44 42 42 37 42 44 42 42 40
 LINE     2     33 36 38 42 44 44 44 42 44 44 44 44 38 39 38 38 44 38 38 38
 LINE     3     36 39 39 40 46 47 40 38 38 43 40 40 43 43 46 40 38 38 40 43
 LINE     4     43 43 43 44 43 43 38 38 43 44 44 44 43 43 44 44 43 43 34 38
 LINE     5     40 44 41 40 41 40 40 41 44 46 46 46 41 44 44 40 35 38 44 40
 LINE     6     32 34 38 38 40 34 34 34 34 34 38 43 43 43 38 40 40 38 34 33
 LINE     7     31 33 35 35 33 35 37 37 40 40 44 42 40 40 42 44 46 44 40 40
 LINE     8     28 30 33 33 33 33 33 36 36 38 38 38 38 38 38 38 38 38 46 46 38
 LINE     9     28 28 28 31 34 34 34 34 38 36 34 31 31 38 40 38 38 38 38 40
 LINE    10     29 29 29 31 33 33 33 34 34 34 33 31 32 34 33 34 38 44 44 38
 LINE    11     30 28 27 31 33 33 35 35 33 31 33 33 33 33 31 31 35 40 37 40
 LINE    12     24 27 27 30 30 35 36 32 35 35 30 32 32 30 32 32 32 36 38 34
 LINE    13     24 27 27 31 35 35 33 33 33 33 31 31 33 33 31 31 33 37 38 37
 LINE    14     23 26 25 32 33 32 33 33 32 33 32 32 32 32 32 32 33 32 32 30
 LINE    15     24 27 28 31 31 31 31 31 31 31 30 30 31 31 30 31 30 31 30 28
 LINE    16     24 24 29 33 31 31 31 31 31 31 31 31 33 31 31 35 31 31 31 31
 LINE    17     23 25 31 34 34 31 30 30 31 30 30 31 34 31 31 31 31 31 30 30
 LINE    18     24 29 30 35 36 30 27 29 30 30 28 30 29 30 30 29 29 29 29 29
 LINE    19     31 31 31 35 40 33 33 29 27 31 29 31 31 31 31 31 29 28 27 29
 LINE    20     30 30 33 38 38 36 38 33 29 28 30 30 32 30 30 30 30 29 29 30
 BAND          5
 LINE     1     27 27 31 29 32 38 38 38 38 38 45 38 38 35 31 38 35 32 35 31
 LINE     2     20 25 27 35 38 42 38 38 38 42 42 38 31 33 30 38 38 31 30 27
 LINE     3     28 27 27 32 43 43 35 32 33 38 38 38 35 35 40 33 32 32 35 40
 LINE     4     37 38 37 41 37 38 37 37 38 38 38 41 38 37 36 38 38 38 26 30
 LINE     5     34 40 38 31 31 34 34 35 38 40 40 40 35 38 38 34 38 28 40 34
 LINE     6     23 28 33 35 33 27 24 24 24 27 28 38 38 38 30 37 37 30 27 27
 LINE     7     22 24 27 27 22 27 31 32 32 32 38 35 35 35 38 38 42 38 35 32
 LINE     8     18 19 25 25 20 23 23 25 27 31 30 30 31 33 33 33 38 46 42 31
 LINE     9     18 18 21 25 22 21 21 25 27 25 22 21 22 32 35 33 27 28 33 33
 LINE    10     18 17 18 22 22 22 25 25 25 24 22 20 24 28 28 28 34 43 41 34
 LINE    11     16 15 16 20 21 23 25 24 24 21 21 21 21 21 20 23 28 35 35 38
 LINE    12     15 16 18 18 22 24 27 23 23 22 20 20 22 20 20 20 20 28 35 32
 LINE    13     14 18 20 22 25 25 22 22 22 20 20 20 20 20 18 20 22 28 25 20
 LINE    14     14 16 19 25 28 18 21 23 21 21 21 21 21 18 18 18 18 18 18 18
 LINE    15     15 16 20 26 21 21 21 20 20 20 21 21 20 20 18 20 20 20 18 18
 LINE    16     14 17 20 24 20 20 18 18 18 18 18 20 20 20 22 18 18 18 18 17
 LINE    17     14 15 24 28 23 21 18 18 20 20 18 20 20 20 20 20 20 18 18 18
 LINE    18     15 20 24 27 28 22 18 18 18 18 18 20 20 20 20 18 20 18 18 18
 LINE    19     22 22 24 31 32 27 25 22 17 18 18 18 18 18 18 18 18 17 17 18
 LINE    20     19 23 28 33 33 35 35 25 18 18 18 18 18 18 18 18 18 18 18 18
 BAND          6
 LINE     1     48 48 45 46 50 48 48 45 48 48 48 45 40 38 35 48 50 45 46 50
 LINE     2     50 47 47 47 47 45 45 44 45 45 45 42 34 34 31 38 45 45 47 50
```

LINE	3	34	36	36	36	34	32	48	46	48	42	42	40	38	40	42	38	36	42	46	48
LINE	4	47	49	49	52	55	49	43	47	47	45	45	43	42	38	42	42	40	40	37	32
LINE	5	41	49	51	49	49	49	43	45	49	46	46	43	43	43	41	35	28	32	43	35
LINE	6	29	32	39	45	41	35	36	38	38	39	36	43	41	38	32	38	36	31	28	28
LINE	7	23	27	32	32	31	40	43	43	43	43	45	45	43	46	40	38	40	43	40	38
LINE	8	20	22	27	29	32	45	50	50	47	44	47	45	40	40	42	44	45	54	50	4
LINE	9	21	20	25	36	48	54	52	52	48	54	52	52	50	42	42	42	40	42	44	4
LINE	10	25	17	18	29	45	50	49	47	47	50	47	47	47	34	32	47	43	43	43	4
LINE	11	24	18	21	38	51	53	45	45	51	53	51	53	53	46	51	51	43	37	37	4
LINE	12	25	22	30	38	45	51	45	45	51	54	49	51	58	54	51	54	49	45	38	3
LINE	13	20	36	36	38	46	46	50	52	52	50	52	56	54	54	54	56	54	45	43	5
LINE	14	14	18	22	31	44	52	52	54	52	52	54	52	54	56	54	52	52	54	54	5
LINE	15	22	33	32	35	46	49	52	52	49	54	58	58	56	58	58	58	58	58	61	6
LINE	16	22	24	34	43	47	51	49	51	51	55	55	55	51	51	55	57	57	57	57	5
LINE	17	13	20	35	43	46	46	45	51	51	51	51	53	55	57	57	57	53	51	53	5
LINE	18	18	28	36	35	33	24	28	47	49	47	47	49	51	51	54	54	54	54	49	5
LINE	19	43	40	40	36	36	32	27	32	45	46	48	50	52	48	52	54	52	49	50	4
LINE	20	50	42	38	36	36	40	40	38	45	48	50	50	50	48	50	48	45	48	50	5
BAND		7																			
LINE	1	22	22	19	23	22	21	18	18	19	19	18	17	15	13	16	21	21	19	20	2
LINE	2	25	23	21	20	20	19	19	19	19	19	19	16	12	12	10	14	16	19	22	2
LINE	3	25	25	26	25	22	21	20	21	20	17	17	16	14	15	16	14	13	17	19	1
LINE	4	20	23	23	22	23	21	19	20	22	19	18	17	16	13	17	16	17	14	15	1
LINE	5	19	21	23	23	22	22	21	20	20	19	19	17	16	15	14	12	10	12	16	1
LINE	6	13	13	18	19	19	15	15	16	16	16	15	18	16	14	11	15	13	12	10	1
LINE	7	9	10	13	13	12	17	20	18	19	19	19	19	18	19	15	15	13	17	19	1
LINE	8	6	8	10	9	14	22	24	24	20	19	21	20	16	18	19	18	18	20	19	1
LINE	9	7	7	10	15	22	24	24	24	22	23	24	25	22	17	16	17	17	17	19	2
LINE	10	9	6	7	13	22	25	24	21	24	24	23	22	21	12	14	20	17	19	19	1
LINE	11	9	5	9	18	25	24	19	21	25	26	25	26	26	22	24	25	19	18	18	1
LINE	12	12	9	12	19	23	25	21	21	25	25	25	25	26	26	25	27	24	20	18	1
LINE	13	9	17	16	19	21	20	23	26	25	24	26	28	28	25	29	27	24	19	20	2
LINE	14	4	6	8	14	19	24	26	26	25	25	28	29	28	25	28	28	24	23	22	2
LINE	15	8	15	14	15	23	25	25	24	24	26	28	26	25	27	25	27	25	23	25	2
LINE	16	10	10	16	19	25	25	25	25	25	27	27	27	28	25	28	28	25	28	28	2
LINE	17	4	8	16	19	23	21	22	24	26	25	25	25	25	27	26	28	25	25	27	2
LINE	18	7	13	16	15	15	10	12	23	25	24	24	25	25	25	25	25	25	23	25	2
LINE	19	20	19	19	16	17	13	12	17	23	24	24	24	24	25	25	25	24	23	24	2
LINE	20	23	19	17	14	15	17	17	18	23	24	24	25	25	24	24	25	24	24	25	2

BAND		4																		
LINE	1	0	0	0	0	0	44	44	44	46	44	44	0	0	37	0	0	0	0	0
LINE	2	0	0	0	44	44	44	42	44	44	44	44	0	0	0	0	44	0	0	0
LINE	3	0	0	0	46	47	0	0	0	43	40	40	0	43	0	40	0	38	40	46
LINE	4	0	0	44	0	0	38	38	0	44	44	44	43	43	44	44	43	0	0	38
LINE	5	44	0	0	0	0	0	0	44	46	46	46	41	0	0	0	0	0	0	0
LINE	6	0	38	38	0	0	0	0	0	0	38	43	43	0	0	40	0	0	0	0
LINE	7	0	0	0	0	0	0	0	0	0	44	42	40	40	0	0	0	44	40	40
LINE	8	0	0	0	0	0	0	0	0	0	0	0	36	38	38	38	38	48	48	38
LINE	9	0	0	0	0	0	0	0	0	0	0	0	0	38	40	38	0	0	38	0
LINE	10	0	0	0	0	0	0	0	0	0	0	0	0	0	33	0	38	44	44	38
LINE	11	0	0	0	0	0	0	0	0	0	0	0	0	0	0	0	0	0	0	40
LINE	12	0	0	0	0	0	0	0	0	0	0	0	0	0	0	0	0	0	0	38
LINE	13	0	0	0	0	0	0	0	0	0	0	0	0	0	0	0	0	0	0	0
LINE	14	0	0	0	0	0	0	0	0	0	0	0	0	0	0	0	0	0	0	0
LINE	15	0	0	0	0	0	0	0	0	0	0	0	0	0	0	0	0	0	0	0
LINE	16	0	0	0	0	0	0	0	0	0	0	0	0	0	0	0	0	0	0	0
LINE	17	0	0	0	0	0	0	0	0	0	0	0	0	0	0	0	0	0	0	0
LINE	18	0	0	0	36	0	0	0	0	0	0	0	0	0	0	0	0	0	0	0
LINE	19	0	0	35	40	0	0	0	0	0	0	0	0	0	0	0	0	0	0	0
LINE	20	0	0	38	38	36	38	0	0	0	0	0	0	0	0	0	0	0	0	0
BAND		5																		

LINE	1	0	0	0	0	0	38	38	39	39	45	38	0	0	31	0	0	0	0	0	0
LINE	2	0	0	0	39	42	38	39	36	42	42	39	0	0	0	0	39	0	0	0	0
LINE	3	0	0	0	43	43	0	0	0	38	38	38	0	38	0	38	0	32	38	40	0
LINE	4	0	0	41	0	0	37	37	0	39	38	4.	38	37	38	38	38	0	0	30	0
LINE	5	40	0	0	0	0	0	0	38	40	40	40	35	0	0	0	0	0	0	0	0
LINE	6	0	33	35	0	0	0	0	0	0	28	38	38	0	0	37	0	0	0	0	0
LINE	7	0	0	0	0	0	0	0	0	0	38	35	35	35	0	0	0	35	35	32	32
LINE	8	0	0	0	0	0	0	0	0	0	0	0	31	33	33	33	38	48	42	31	31
LINE	9	0	0	0	0	0	0	0	0	0	0	0	0	32	35	33	0	0	33	0	0
LINE	10	0	0	0	0	0	0	0	0	0	0	0	0	0	28	0	34	43	41	34	0
LINE	11	0	0	0	0	0	0	0	0	0	0	0	0	0	0	0	0	0	0	29	0
LINE	12	0	0	0	0	0	0	0	0	0	0	0	0	0	0	0	0	0	0	32	0
LINE	13	0	0	0	0	0	0	0	0	0	0	0	0	0	0	0	0	0	0	0	0
LINE	14	0	0	0	0	0	0	0	0	0	0	0	0	0	0	0	0	0	0	0	0
LINE	15	0	0	0	0	0	0	0	0	0	0	0	0	0	0	0	0	0	0	0	0
LINE	16	0	0	0	0	0	0	0	0	0	0	0	0	0	0	0	0	0	0	0	0
LINE	17	0	0	0	0	0	0	0	0	0	0	0	0	0	0	0	0	0	0	0	0
LINE	18	0	0	0	28	0	0	0	0	0	0	0	0	0	0	0	0	0	0	0	0
LINE	19	0	0	31	32	0	0	0	0	0	0	0	0	0	0	0	0	0	0	0	0
LINE	20	0	0	33	33	35	35	0	0	0	0	0	0	0	0	0	0	0	0	0	0
BAND		6																			
LINE	1	0	0	0	0	0	46	45	46	48	48	45	0	0	38	0	0	0	0	0	0
LINE	2	0	0	0	47	45	45	44	45	45	45	42	0	0	0	0	45	0	0	0	0
LINE	3	0	0	0	52	52	0	0	0	42	42	40	0	40	0	38	0	42	45	43	0
LINE	4	0	0	52	0	0	43	47	0	45	45	43	42	38	42	42	40	0	0	32	0
LINE	5	49	0	0	0	0	0	0	49	46	46	43	43	0	0	0	0	0	0	0	0
LINE	6	0	39	45	0	0	0	0	0	0	38	43	41	0	0	38	0	0	0	0	0
LINE	7	0	0	0	0	0	0	0	0	0	45	45	43	43	0	0	0	43	43	38	38
LINE	8	0	0	0	0	0	0	0	0	0	0	0	40	40	42	44	45	54	50	42	38
LINE	9	0	0	0	0	0	0	0	0	0	0	0	0	42	42	44	0	0	44	0	0
LINE	10	0	0	0	0	0	0	0	0	0	0	0	0	0	32	0	43	43	43	40	0
LINE	11	0	0	0	0	0	0	0	0	0	0	0	0	0	0	0	0	0	0	41	0
LINE	12	0	0	0	0	0	0	0	0	0	0	0	0	0	0	0	0	0	0	38	0
LINE	13	0	0	0	0	0	0	0	0	0	0	0	0	0	0	0	0	0	0	0	0
LINE	14	0	0	0	0	0	0	0	0	0	0	0	0	0	0	0	0	0	0	0	0
LINE	15	0	0	0	0	0	0	0	0	0	0	0	0	0	0	0	0	0	0	0	0
LINE	16	0	0	0	0	0	0	0	0	0	0	0	0	0	0	0	0	0	0	0	0
LINE	17	0	0	0	0	0	0	0	0	0	0	0	0	0	0	0	0	0	0	0	0
LINE	18	0	0	0	33	0	0	0	0	0	0	0	0	0	0	0	0	0	0	0	0
LINE	19	0	0	36	36	0	0	0	0	0	0	0	0	0	0	0	0	0	0	0	0
LINE	20	0	0	36	36	40	40	0	0	0	0	0	0	0	0	0	0	0	0	0	0
BAND		7																			
LINE	1	0	0	0	0	0	18	19	19	19	19	17	0	0	16	0	0	0	0	0	0
LINE	2	0	0	0	20	19	19	19	19	19	19	16	0	0	0	0	19	0	0	0	0
LINE	3	0	0	0	22	21	0	0	0	17	17	16	0	15	0	14	0	17	16	17	0
LINE	4	0	0	22	0	0	19	20	0	19	18	17	16	16	17	16	17	0	0	14	0
LINE	5	21	0	0	0	0	0	0	20	19	18	17	16	0	0	0	0	0	0	0	0
LINE	6	0	18	19	0	0	0	0	0	0	15	19	16	0	0	15	0	0	0	0	0
LINE	7	0	0	0	0	0	0	0	0	0	19	18	18	19	0	0	0	17	16	16	16
LINE	8	0	0	0	0	0	0	0	0	0	0	0	16	16	18	18	19	20	19	16	16
LINE	9	0	0	0	0	0	0	0	0	0	0	0	0	17	16	17	0	0	16	0	0
LINE	10	0	0	0	0	0	0	0	0	0	0	0	0	0	14	0	17	18	18	17	0
LINE	11	0	0	0	0	0	0	0	0	0	0	0	0	0	0	0	0	0	0	17	0
LINE	12	0	0	0	0	0	0	0	0	0	0	0	0	0	0	0	0	0	0	15	0
LINE	13	0	0	0	0	0	0	0	0	0	0	0	0	0	0	0	0	0	0	0	0
LINE	14	0	0	0	0	0	0	0	0	0	0	0	0	0	0	0	0	0	0	0	0
LINE	15	0	0	0	0	0	0	0	0	0	0	0	0	0	0	0	0	0	0	0	0
LINE	16	0	0	0	0	0	0	0	0	0	0	0	0	0	0	0	0	0	0	0	0
LINE	17	0	0	0	0	0	0	0	0	0	0	0	0	0	0	0	0	0	0	0	0
LINE	18	0	0	0	15	0	0	0	0	0	0	0	0	0	0	0	0	0	0	0	0
LINE	19	0	0	16	17	0	0	0	0	0	0	0	0	0	0	0	0	0	0	0	0
LINE	20	0	0	14	15	17	17	0	0	0	0	0	0	0	0	0	0	0	0	0	0

S T A T I S T I C A L A N A L Y S I S S Y S T E M

VARIABLE	N	MEAN	STANDARD DEVIATION	VARIANCE	MINIMUM VALUE	MAXIMUM VALUE	RANGE
B41	324	34.65740741	2.90881665	8.46121431	28.00000000	44.00000000	16.00000000
B51	324	28.16666667	3.87777664	15.03715170	16.00000000	43.00000000	27.00000000
B61	324	34.75000000	4.77958442	22.84442724	23.00000000	47.00000000	24.00000000
B71	324	15.47530864	2.57566756	6.63406337	11.00000000	22.00000000	11.00000000
B42	324	39.89814815	4.65451573	21.66451668	26.00000000	49.00000000	23.00000000
B52	324	34.25925926	5.06374909	25.64155487	19.00000000	48.00000000	29.00000000
B62	324	41.79320988	5.83178678	34.00973703	26.00000000	54.00000000	28.00000000
B72	324	17.49382716	2.64574409	6.99996178	12.00000000	23.00000000	11.00000000

S T A T I S T I C A L A N A L Y S I S S Y S T E M

VARIABLE	N	MEAN	STANDARD DEVIATION	VARIANCE	MINIMUM VALUE	MAXIMUM VALUE	RANGE
B4C	324	34.65745278	2.90860688	8.45999398	25.97250000	40.34520000	14.37270000
B5C	324	28.16664074	3.87781905	15.03748062	16.48110000	38.68930000	22.20820000
B6C	324	34.75001481	4.77973244	22.84584224	21.80590000	44.75470000	22.94880000
B7C	324	15.47528889	2.29782874	5.28001692	10.70390000	20.25740000	9.55350000

S T A T I S T I C A L A N A L Y S I S S Y S T E M

VARIABLE	N	MEAN	STANDARD DEVIATION	VARIANCE	MINIMUM VALUE	MAXIMUM VALUE	RANGE
B4E	324	34.65611204	2.80993115	7.89571305	26.26580000	40.15090000	13.88510000
B5E	324	28.16591852	3.79730544	14.41952864	16.72300000	38.47010000	21.74710000
B6E	324	34.74798025	4.58611712	21.03247026	22.32820000	44.34740000	22.01920000
B7E	324	15.47541852	2.49943444	6.24717252	10.28540000	20.67710000	10.39170000

Table 4. Listing of means, standard deviations, and variances.

where, E denotes image 2's PIF's data set transformed using the values determined from the regression analysis,

and, C denotes image 2's data set transformed using the values determined from the LHAO (bands 4 through 7).

S T A T I S T I C A L A N A L Y S I S S Y S T E M

FREQUENCY BAR CHART

B41

brightness value		FREQ	CUM. FREQ	PERCENT	CUM. PERCENT
28	****	4	4	1.23	1.23
29	*********	9	13	2.78	4.01
30	******************	18	31	5.56	9.57
31	************	12	43	3.70	13.27
32	******************	18	61	5.56	18.83
33	**	49	110	15.12	33.95
34	***	44	154	13.58	47.53
35	**	68	222	20.99	68.52
36	********************	20	242	6.17	74.69
37	************************	24	266	7.41	82.10
38	*****************************	28	294	8.64	90.74
39	************	13	307	4.01	94.75
40	*********	9	316	2.78	97.53
41	*****	5	321	1.54	99.07
43	*	1	322	0.31	99.38
44	**	2	324	0.62	100.00

5 10 15 20 25 30 35 40 45 50 55 60 65

FREQUENCY

Figure 3. Frequency vs brightness value for image 1, band 4.

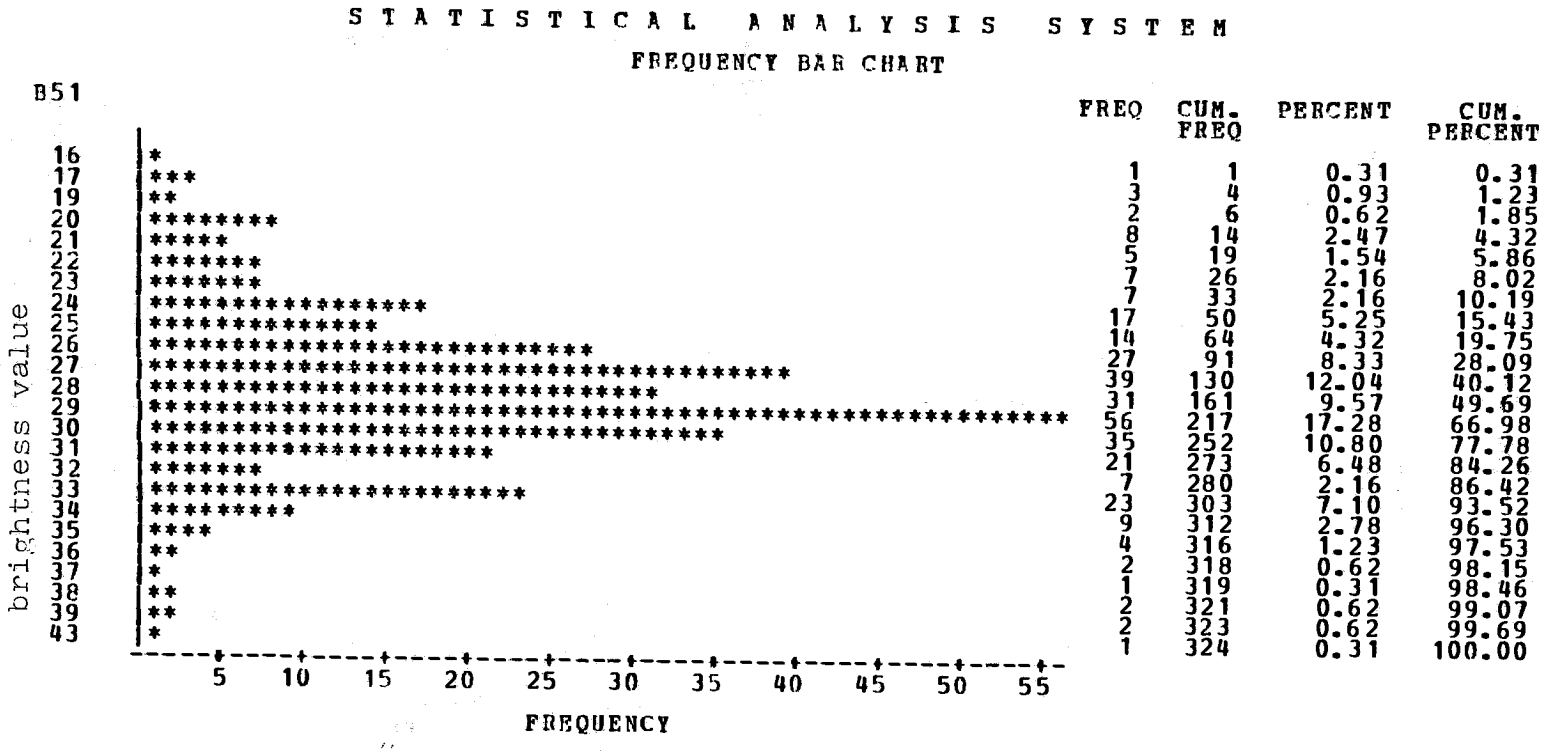

Figure 4. Frequency vs brightness value for image 1, band 5.

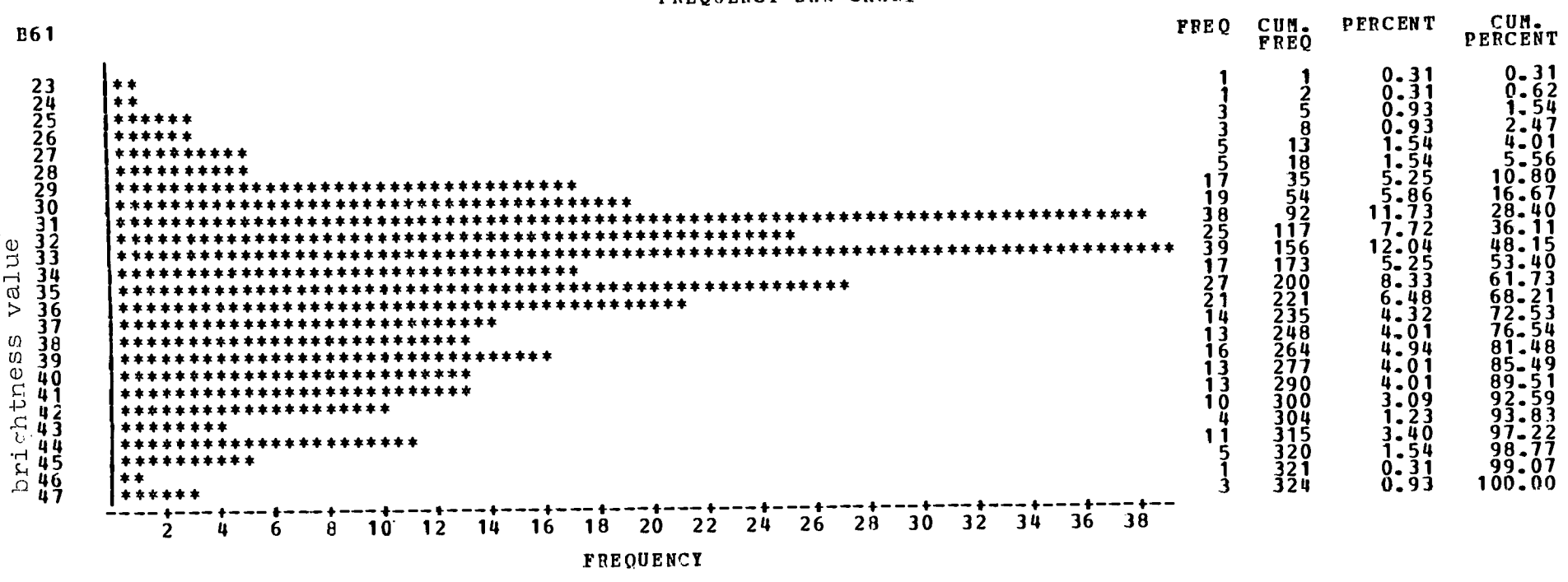

Figure 5. Frequency vs brightness value for image 1, band 6.

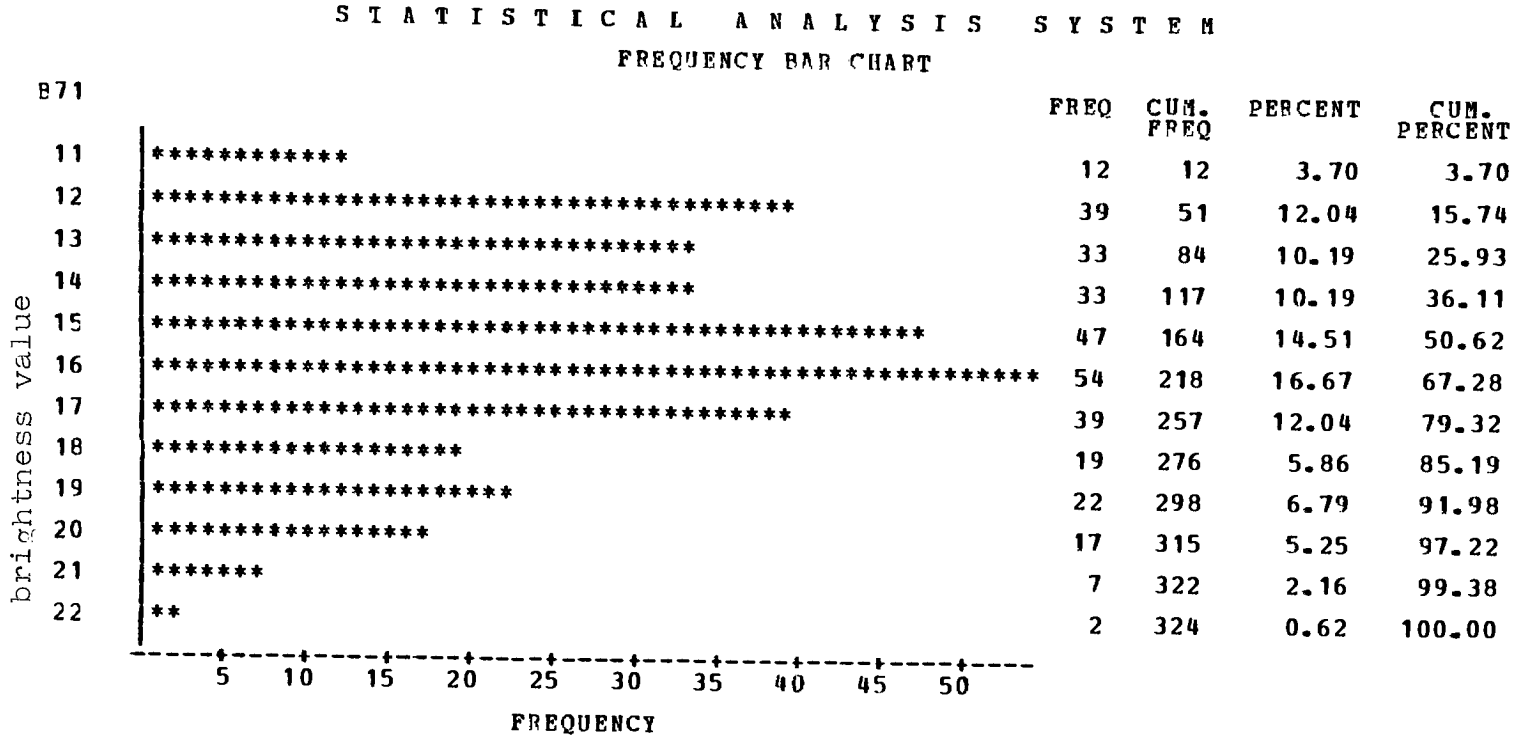

Figure 6. Frequency vs brightness value for image 1, band 7.

S T A T I S T I C A L A N A L Y S I S S Y S T E M

FREQUENCY BAR CHART

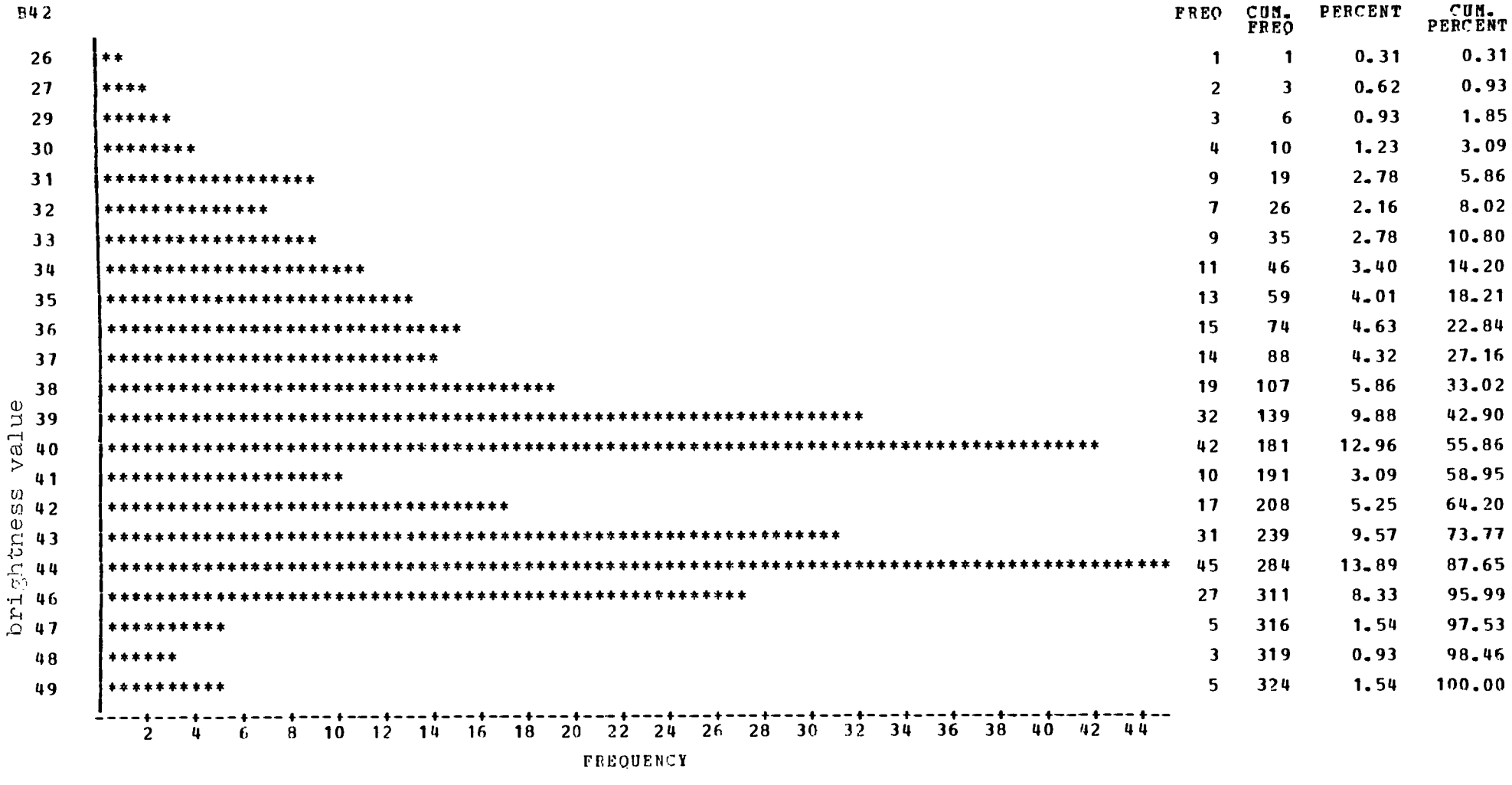

Figure 7. Frequency vs brightness value for image 2, band 4.

S T A T I S T I C A L A N A L Y S I S S Y S T E M

FREQUENCY BAR CHART

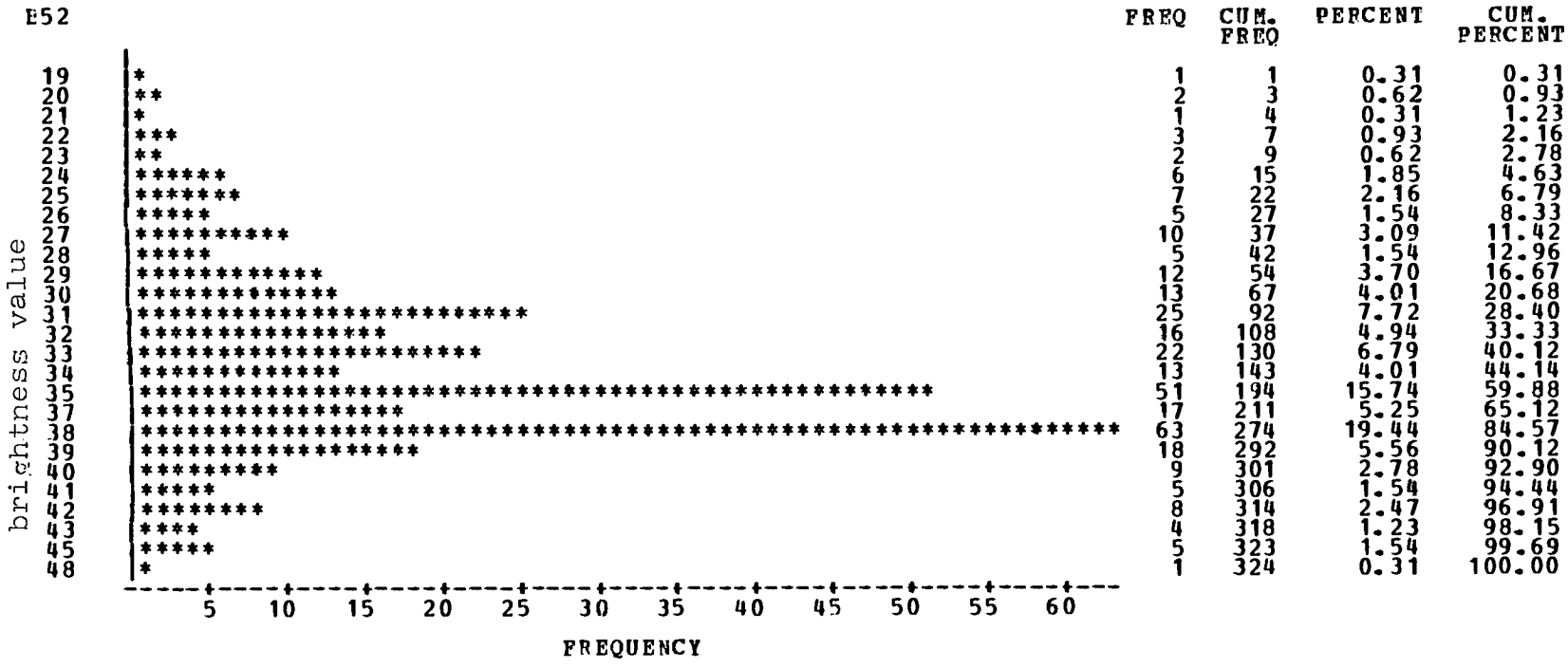

	FREQ	CUM. FREQ	PERCENT	CUM. PERCENT
19	1	1	0.31	0.31
20	2	3	0.62	0.93
21	1	4	0.31	1.23
22	3	7	0.93	2.16
23	2	9	0.62	2.78
24	6	15	1.85	4.63
25	7	22	2.16	6.79
26	5	27	1.54	8.33
27	10	37	3.09	11.42
28	5	42	1.54	12.96
29	12	54	3.70	16.67
30	13	67	4.01	20.68
31	25	92	7.72	28.40
32	16	108	4.94	33.33
33	22	130	6.79	40.12
34	13	143	4.01	44.14
35	51	194	15.74	59.88
37	17	211	5.25	65.12
38	63	274	19.44	84.57
39	18	292	5.56	90.12
40	9	301	2.78	92.90
41	5	306	1.54	94.44
42	8	314	2.47	96.91
43	4	318	1.23	98.15
45	5	323	1.54	99.69
48	1	324	0.31	100.00

Figure 8. Frequency vs brightness value for image 2, band 5.

S T A T I S T I C A L A N A L Y S I S S Y S T E M

FREQUENCY BAR CHART

B62

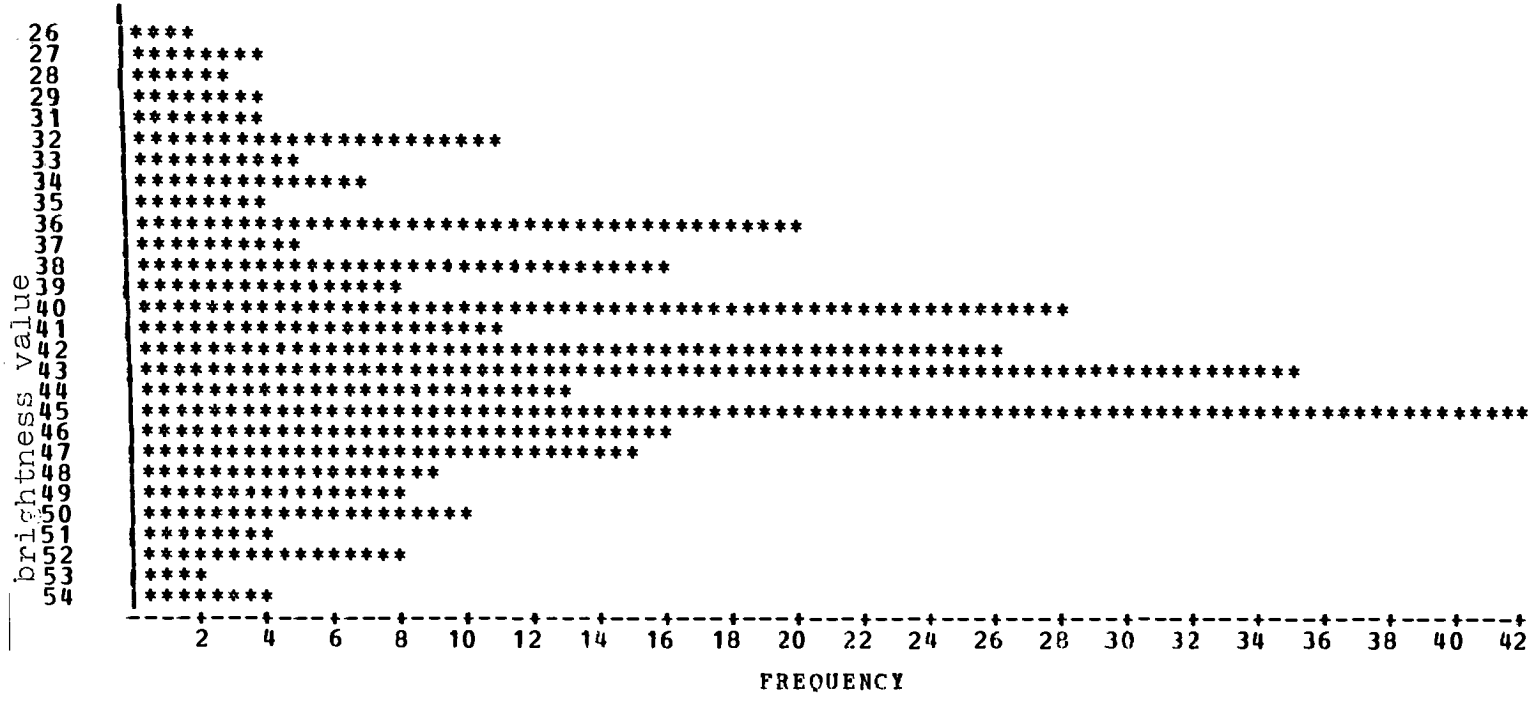

	FREQ	CUM. FREQ	PERCENT	CUM. PERCENT
26	2	2	0.62	0.62
27	4	6	1.23	1.85
28	3	9	0.93	2.78
29	4	13	1.23	4.01
31	4	17	1.23	5.25
32	11	28	3.40	8.64
33	5	33	1.54	10.19
34	7	40	2.16	12.35
35	4	44	1.23	13.58
36	20	64	6.17	19.75
37	5	69	1.54	21.30
38	16	85	4.94	26.23
39	8	93	2.47	28.70
40	28	121	8.64	37.35
41	11	132	3.40	40.74
42	26	158	8.02	48.77
43	35	193	10.80	59.57
44	13	206	4.01	63.58
45	42	248	12.96	76.54
46	16	264	4.94	81.48
47	15	279	4.63	86.11
48	9	288	2.78	88.89
49	8	296	2.47	91.36
50	10	306	3.09	94.44
51	4	310	1.23	95.68
52	8	318	2.47	98.15
53	2	320	0.62	98.77
54	4	324	1.23	100.00

Figure 9. Frequency vs brightness value for image 2, band 6.

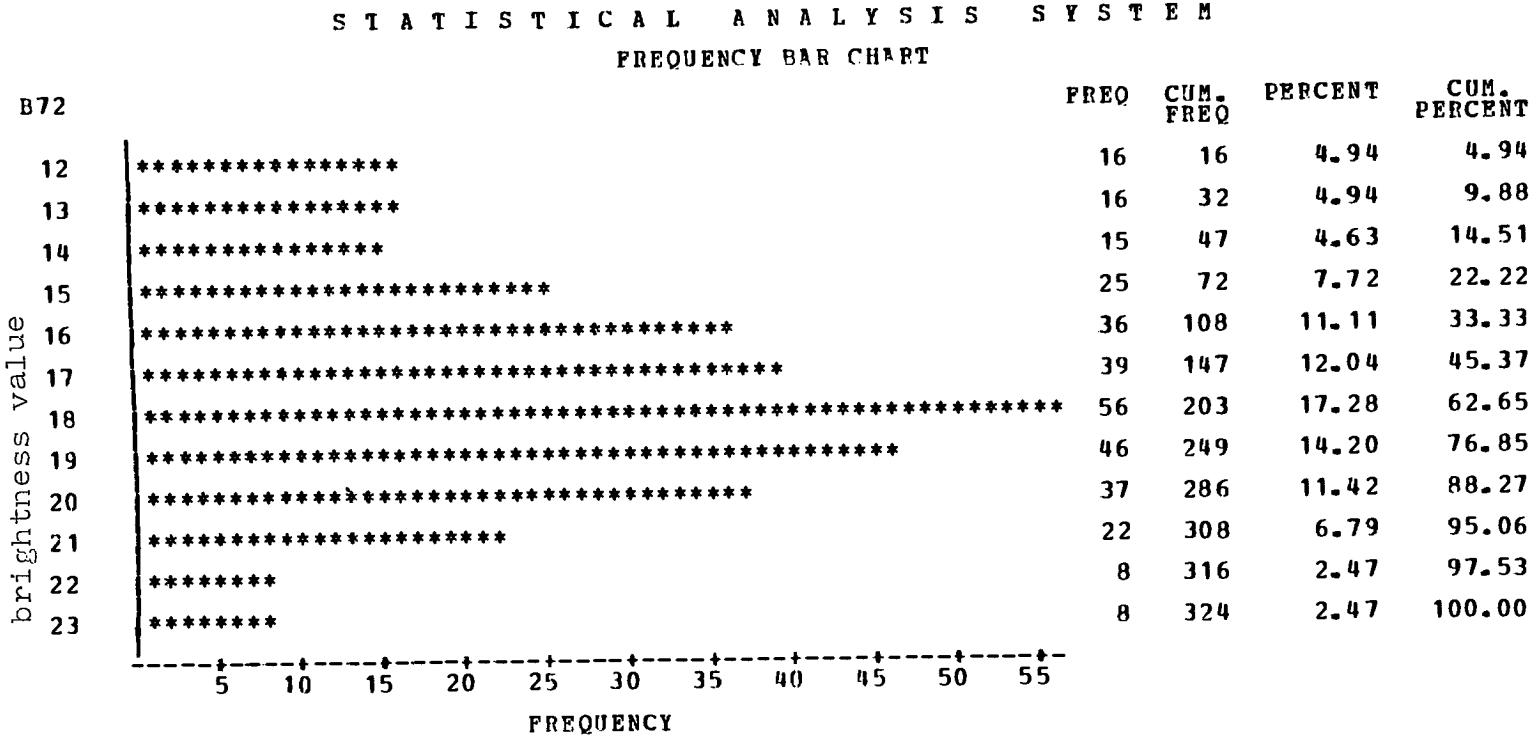

	FREQ	CUM. FREQ	PERCENT	CUM. PERCENT
12	16	16	4.94	4.94
13	16	32	4.94	9.88
14	15	47	4.63	14.51
15	25	72	7.72	22.22
16	36	108	11.11	33.33
17	39	147	12.04	45.37
18	56	203	17.28	62.65
19	46	249	14.20	76.85
20	37	286	11.42	88.27
21	22	308	6.79	95.06
22	8	316	2.47	97.53
23	8	324	2.47	100.00

Figure 10. Frequency vs brightness value for image 2, band 7.

S T A T I S T I C A L A N A L Y S I S S Y S T E M

FREQUENCY BAR CHART

B4C		FREQ	CUM. FREQ	PERCENT	CUM. PERCENT
25.9725	**	1	1	0.31	0.31
26.5974	****	2	3	0.62	0.93
27.8472	******	3	6	0.93	1.85
28.4721	********	4	10	1.23	3.09
29.0970	******************	9	19	2.78	5.86
29.7219	**************	7	26	2.16	8.02
30.3468	******************	9	35	2.78	10.80
30.9717	**********************	11	46	3.40	14.20
31.5966	**************************	13	59	4.01	18.21
32.2215	******************************	15	74	4.63	22.84
32.8464	*****************************	14	88	4.32	27.16
33.4713	************************************	19	107	5.86	33.02
34.0962	**	32	139	9.88	42.90
34.7211	**	42	181	12.96	55.86
35.3460	********************	10	191	3.09	58.95
35.9709	**********************************	17	208	5.25	64.20
36.5958	**	31	239	9.57	73.77
37.2207	**	45	284	13.89	87.65
38.4705	***	27	311	8.33	95.99
39.0954	**********	5	316	1.54	97.53
39.7203	******	3	319	0.93	98.46
40.3452	**********	5	324	1.54	100.00

2 4 6 8 10 12 14 16 18 20 22 24 26 28 30 32 34 36 38 40 42 44

FREQUENCY

Figure 11. Frequency vs brightness value for image 2 transformed using the slope and intercept derived from the LHAO method (band 4).

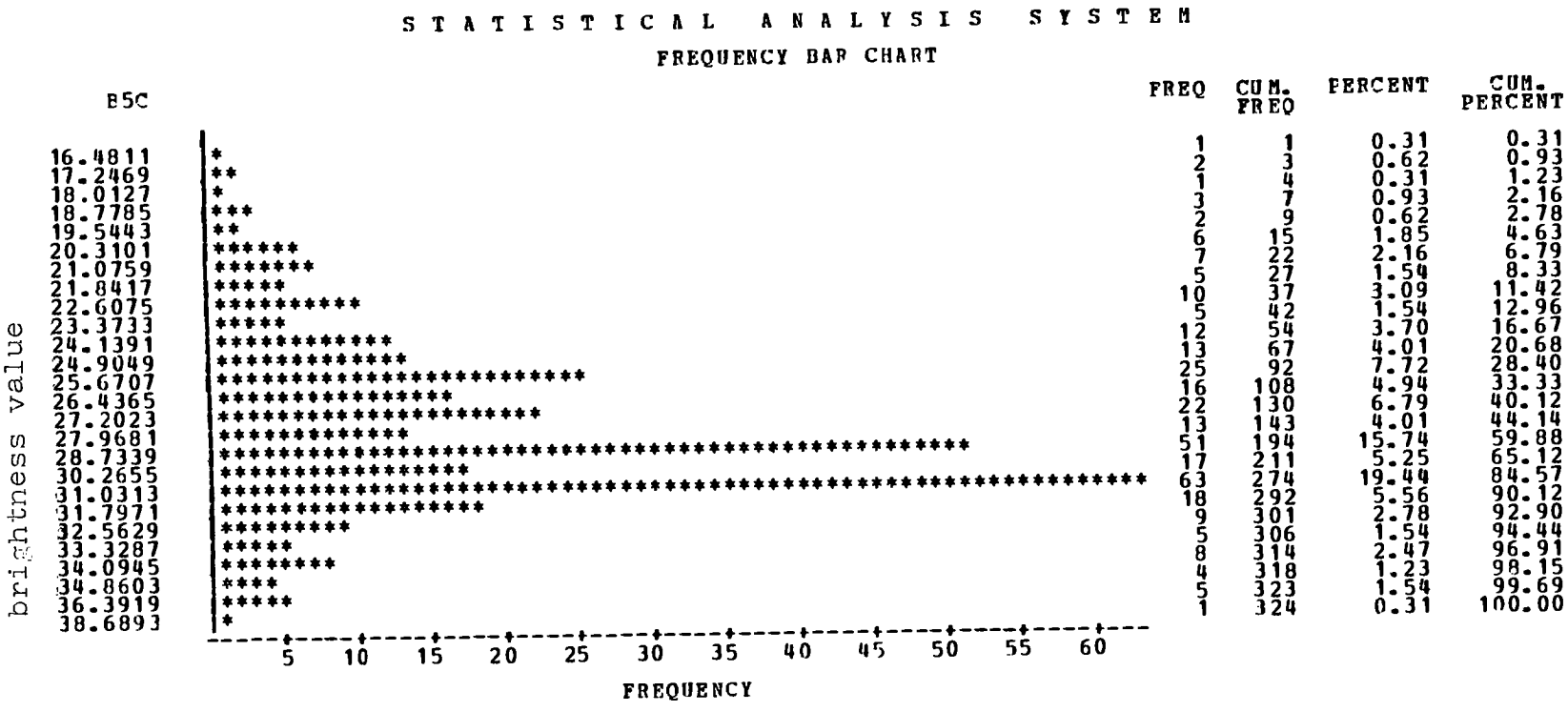

Figure 12. Frequency vs brightness value for image 2 transformed using the slope and intercept derived from the LHAO method (band 5).

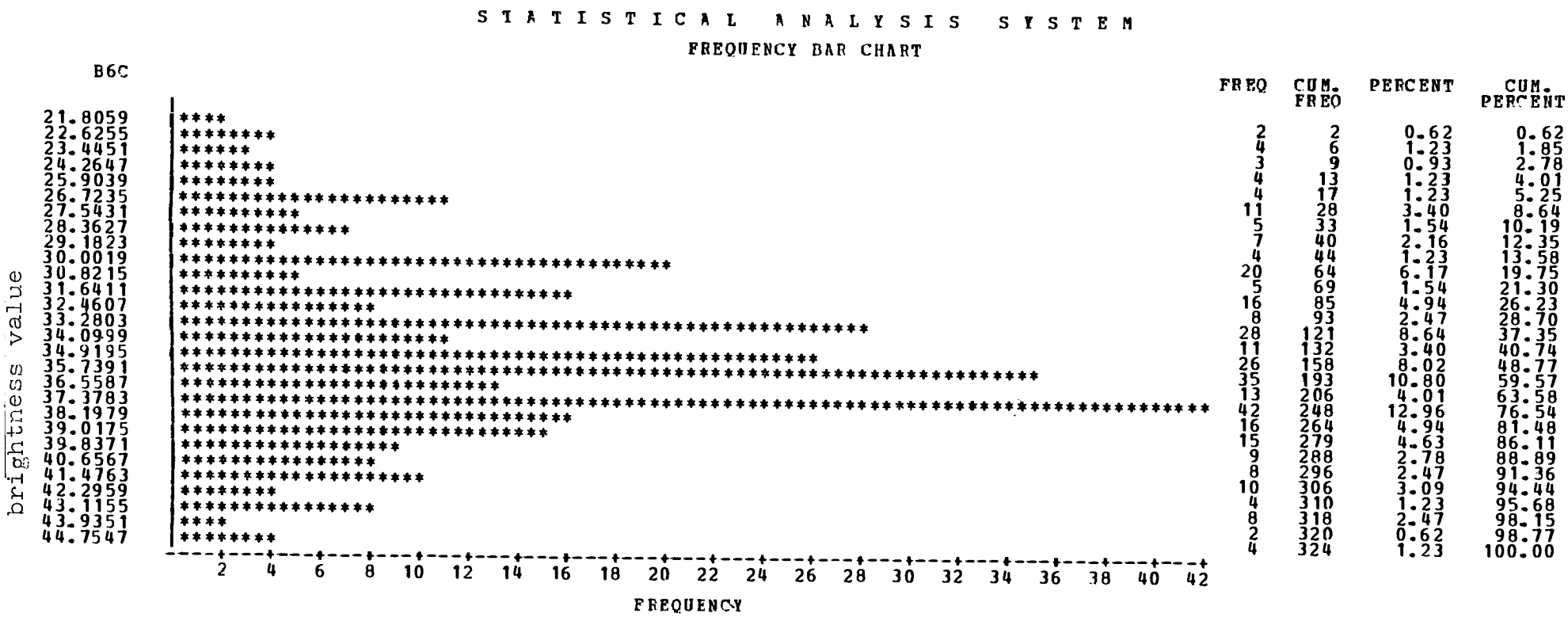

Figure 13. Frequency vs brightness value for image 2 transformed using the slope and intercept derived from the LHAO method (band 6).

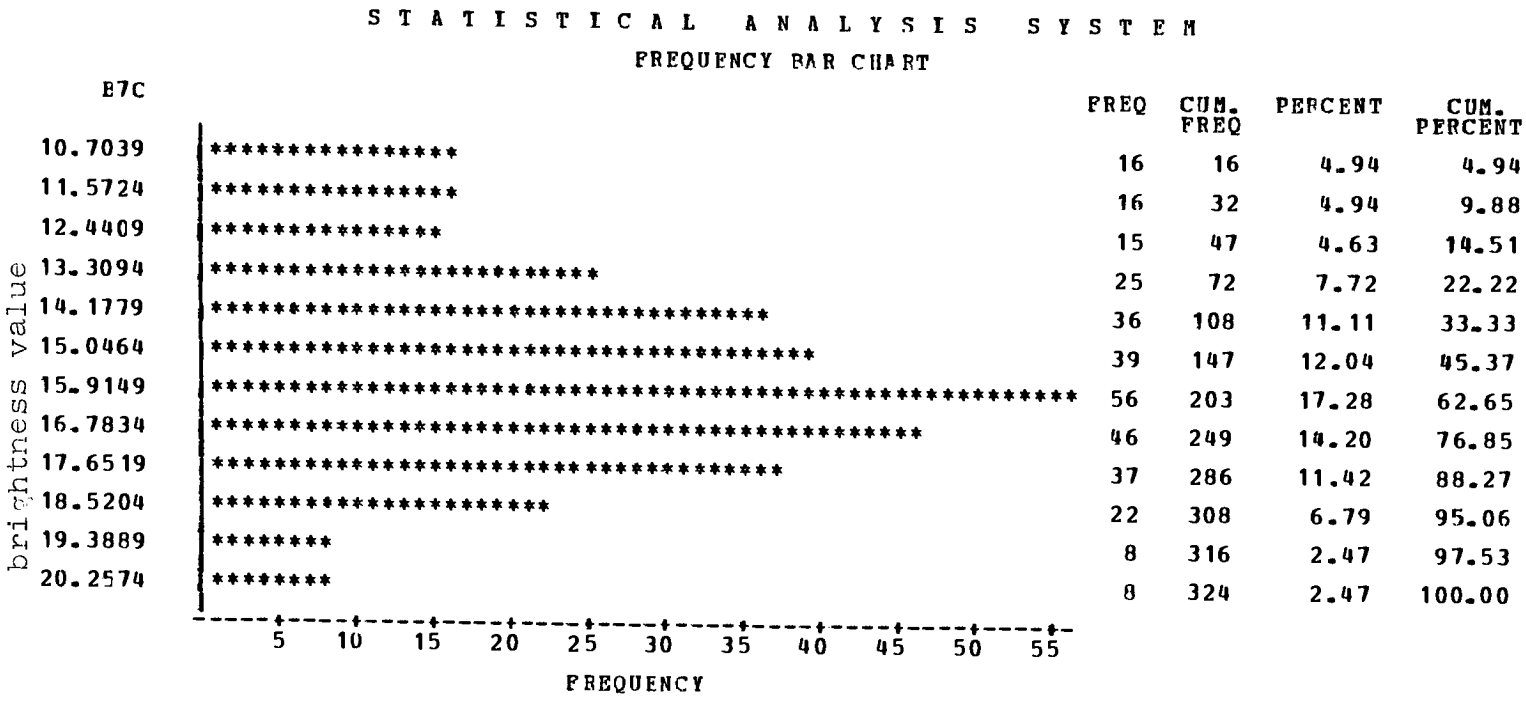

Figure 14. Frequency vs brightness value for image 2 transformed using the slope and intercept derived from the LHAO method (band 7).

S T A T I S T I C A L A N A L Y S I S S Y S T E M

FREQUENCY BAR CHART

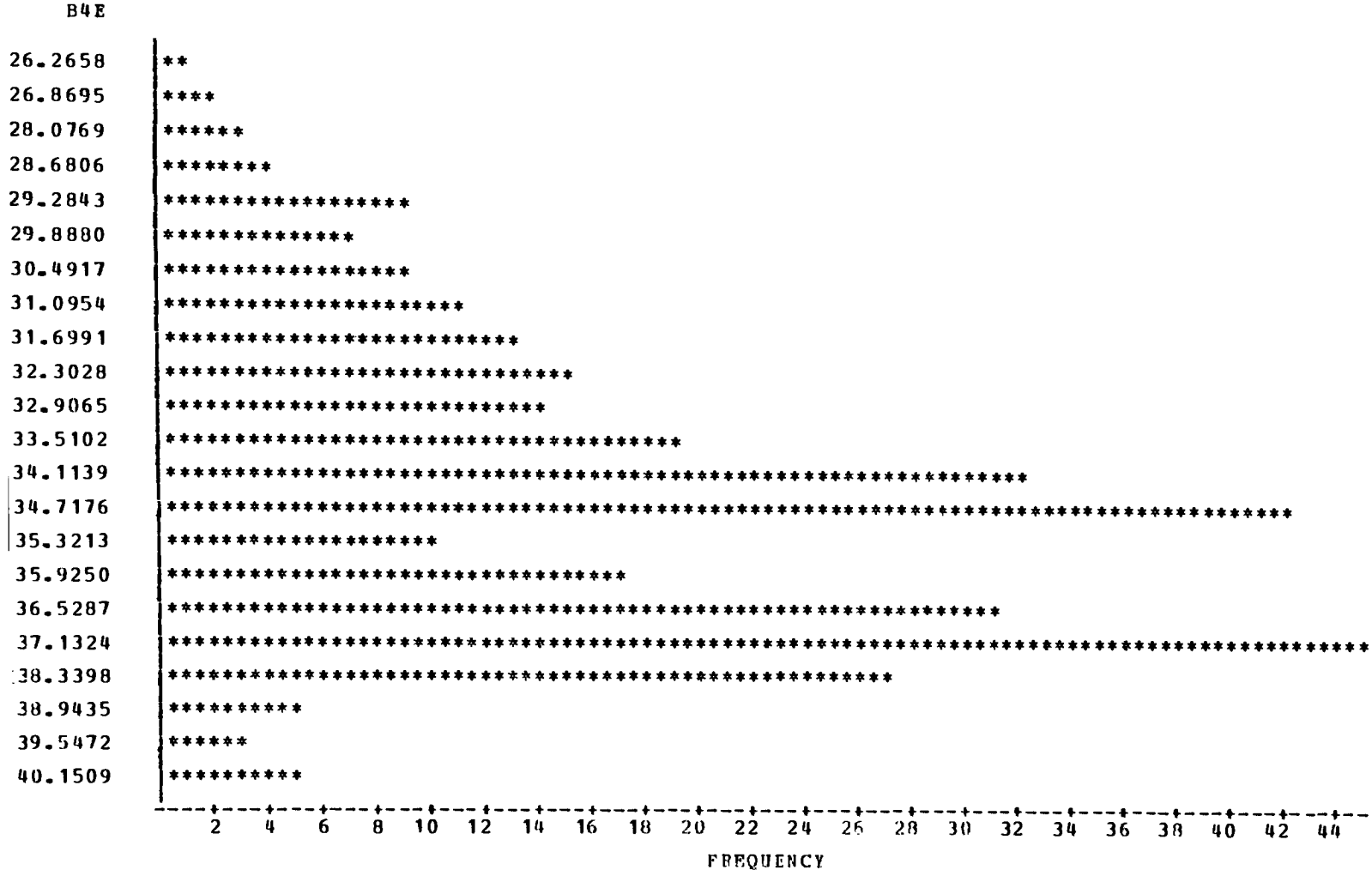

	FREQ	CUM. FREQ	PERCENT	CUM. PERCENT
26.2658	1	1	0.31	0.31
26.8695	2	3	0.62	0.93
28.0769	3	6	0.93	1.85
28.6806	4	10	1.23	3.09
29.2843	9	19	2.78	5.86
29.8880	7	26	2.16	8.02
30.4917	9	35	2.78	10.80
31.0954	11	46	3.40	14.20
31.6991	13	59	4.01	18.21
32.3028	15	74	4.63	22.84
32.9065	14	88	4.32	27.16
33.5102	19	107	5.86	33.02
34.1139	32	139	9.88	42.90
34.7176	42	181	12.96	55.86
35.3213	10	191	3.09	58.95
35.9250	17	208	5.25	64.20
36.5287	31	239	9.57	73.77
37.1324	45	284	13.89	87.65
38.3398	27	311	8.33	95.99
38.9435	5	316	1.54	97.53
39.5472	3	319	0.93	98.46
40.1509	5	324	1.54	100.00

Figure 15. Frequency vs brightness value for image 2 transformed using the slope and intercept calculated by the regression analysis (band 4).

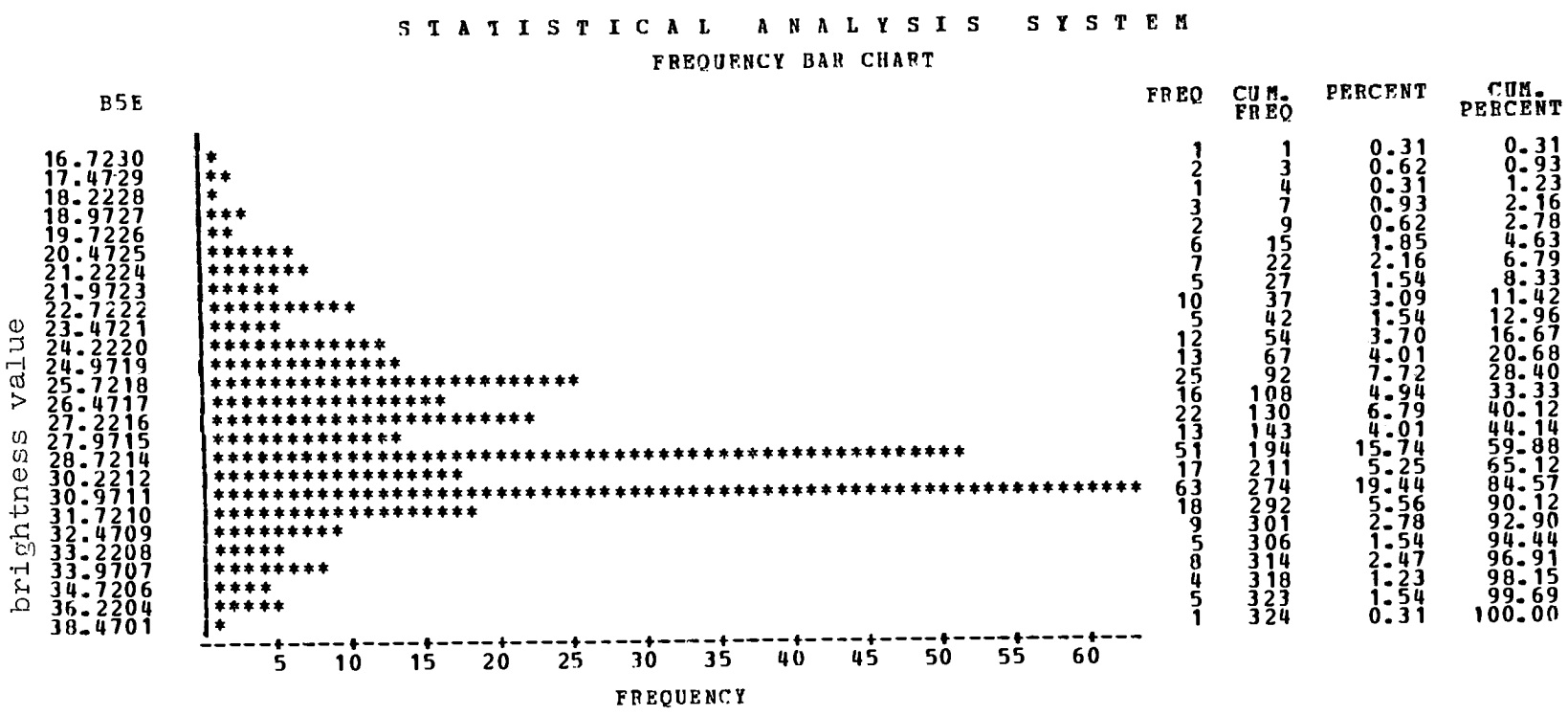

Figure 16. Frequency vs brightness value for image 2 transformed using the slope and intercept calculated by the regression analysis (band 5).

S T A T I S T I C A L A N A L Y S I S S Y S T E M

FREQUENCY BAR CHART

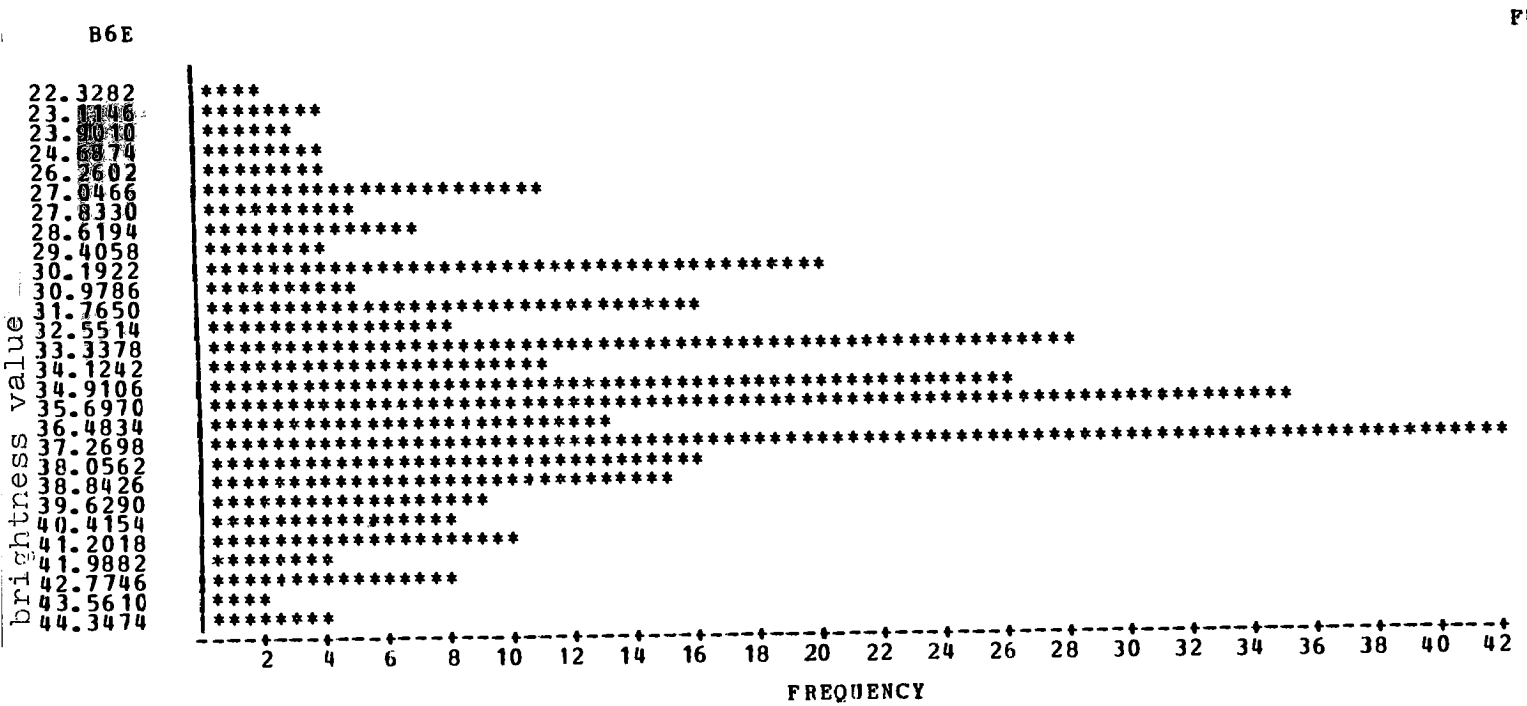

	FREQ	CUM. FREQ	PERCENT	CUM. PERCENT
22.3282	2	2	0.62	0.62
23.1146	4	6	1.23	1.85
23.9010	3	9	0.93	2.78
24.6874	4	13	1.23	4.01
26.2602	4	17	1.23	5.25
27.0466	11	28	3.40	8.64
27.8330	5	33	1.54	10.19
28.6194	7	40	2.16	12.35
29.4058	4	44	1.23	13.58
30.1922	20	64	6.17	19.75
30.9786	5	69	1.54	21.30
31.7650	16	85	4.94	26.23
32.5514	8	93	2.47	28.70
33.3378	28	121	8.64	37.35
34.1242	11	132	3.40	40.74
34.9106	26	158	8.02	48.77
35.6970	35	193	10.80	59.57
36.4834	13	206	4.01	63.58
37.2698	42	248	12.96	76.54
38.0562	16	264	4.94	81.48
38.8426	15	279	4.63	86.11
39.6290	9	288	2.78	88.89
40.4154	8	296	2.47	91.36
41.2018	10	306	3.09	94.44
41.9882	4	310	1.23	95.68
42.7746	8	318	2.47	98.15
43.5610	2	320	0.62	98.77
44.3474	4	324	1.23	100.00

Figure 17. Frequency vs brightness value for image 2 transformed using the slope and intercept calculated by the regression analysis (band 6).

S T A T I S T I C A L A N A L Y S I S S Y S T E M

FREQUENCY BAR CHART

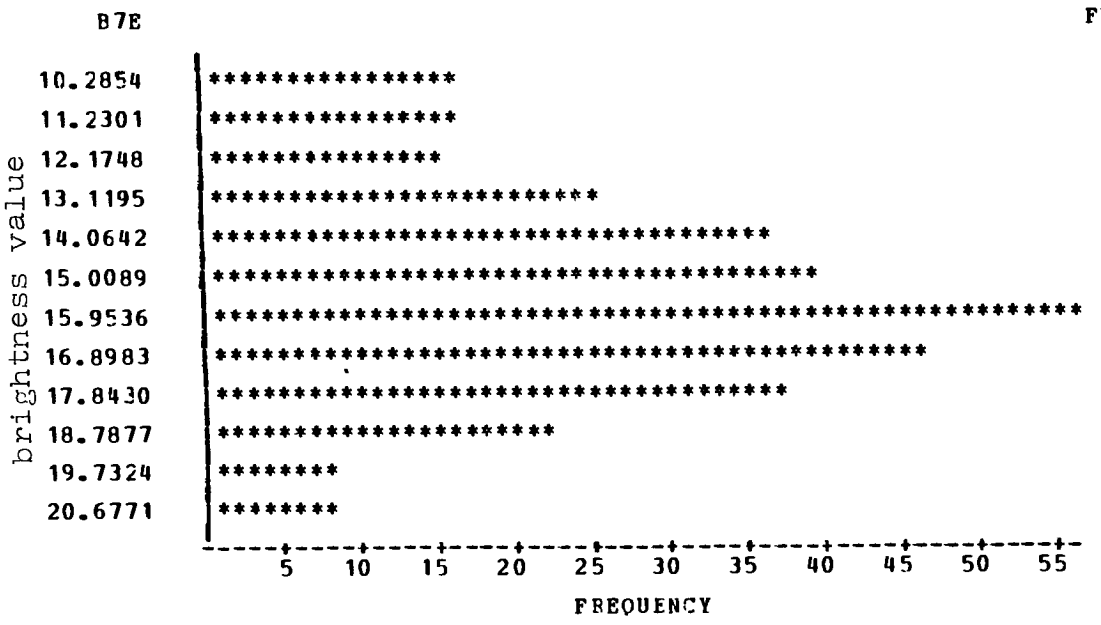

	FREQ	CUM. FREQ	PERCENT	CUM. PERCENT
10.2854	16	16	4.94	4.94
11.2301	16	32	4.94	9.88
12.1748	15	47	4.63	14.51
13.1195	25	72	7.72	22.22
14.0642	36	108	11.11	33.33
15.0089	39	147	12.04	45.37
15.9536	56	203	17.28	62.65
16.8983	46	249	14.20	76.85
17.8430	37	286	11.42	88.27
18.7877	22	308	6.79	95.06
19.7324	8	316	2.47	97.53
20.6771	8	324	2.47	100.00

Figure 18. Frequency vs brightness value for image 2 transformed using the slope and intercept calculated by the regression analysis (band 7).

XI. VITA

The author was born in New York City in 1959. He grew up on Long Island, and attended Floral Park Memorial High School after which he attended college at S.U.N.Y at Farmingdale where he obtained his Associate Degree in Photographic Technology. He then attended Rochester Institute of Technology, where apon graduation he will obtain his Bachelor of Science Degree in Photographic Science and Instrumentation.

In the future the author will pursue a Masters Degree in either Computer Science or Statistics.